Draft NISTIR xxxx
(For Public Comment)

Face Recognition Vendor Test (FRVT) MORPH
Performance of Automated Face Morph Detection

Mei Ngan
Patrick Grother
Kayee Hanaoka
Information Access Division
Information Technology Laboratory

This publication is available free of charge from:
https://doi.org/10.6028/NIST.IR.xxxx

NIST
National Institute of
Standards and Technology
U.S. Department of Commerce

Draft NISTIR xxxx
(For Public Comment)

Face Recognition Vendor Test (FRVT) MORPH
Performance of Automated Face Morph Detection

Mei Ngan
Patrick Grother
Kayee Hanaoka
Information Access Division
Information Technology Laboratory

This publication is available free of charge from:
https://doi.org/10.6028/NIST.IR.xxxx

Last Updated: September 18, 2019

U.S. Department of Commerce
Wilbur L. Ross, Jr., Secretary

National Institute of Standards and Technology
Walter Copan, NIST Director and Under Secretary of Commerce for Standards and Technology

FRVT MORPH Status and Changelog

This report is a draft NIST Interagency Report, and is open for comment until October 31, 2019. This report will be updated as new algorithms are evaluated, as new datasets are added, and as new analyses are included. Comments and suggestions should be directed to frvt@nist.gov.

Executive Summary

Background

Face morphing and the ability to detect it is an area of high interest to a number of photo-credential issuance agencies, companies, and organizations employing face recognition for identity verification. Face morphing is an image manipulation technique where two or more subjects' faces are morphed or blended together to form a single face in a photograph. Morphed photos can look very realistically like all contributing subjects. Morphing is easy to do and requires little to no technical experience given the vast availability of tools available at little or no cost on the internet and mobile platforms. If a morphed photo gets onto an identity credential for example, multiple, if not all constituents of the morph, can use the same identity credential. Morphs can be used to fool both humans [1] [2] and current face recognition systems [3], such as those deployed in Automatic Border Control gates or eGates, which presents a vulnerability to current identity verification processes.

FRVT MORPH Test Activity

The FRVT MORPH test provides ongoing independent testing of prototype face morph detection technologies. The evaluation is designed to obtain commonly measured assessment of morph detection capability to inform developers and current and prospective end-users. FRVT MORPH is open for ongoing participation worldwide, and there is no charge to participate. The test opened in June 2018, and NIST has since received five morph detection algorithm submissions from three academic entities - Hochschule Darmstadt University of Applied Sciences, Norwegian University of Science and Technology, and University of Bologna.

The test leverages a number of datasets created using different morphing methods with goals to evaluate algorithm performance over a large spectrum of morphing techniques. Testing was conducted using a tiered approach, where algorithms were evaluated on low quality morphs created with readily accessible tools available to non-experts, morphs generated using automated morphing methods based on academic research, and high quality morphs created using commercial-grade tools. We'd like to get an assessment on the existence and extent of morph detection capabilities, and if there is indication of high accuracy, much larger datasets can be curated to support large-scale evaluation of the technology.

Results and Notable Observations

Ideally, it is important that morph detection technology produce very low false detection rates given the assumption that most transactions (for passport applications or at an eGate for example) will be on legitimate photos that are not morphs. False detection rates need to be controlled, because additional amounts of resources will be required to adjudicate such errors. With that said, an initial automated morph detection capability with say ideally 0% false detection rates but high morph miss rates would still yield gains in operations compared to not having any morph detection capability at all.

- **Single-image Morph Detection:** In this use case, a single image is provided to the algorithm, and the software has to 1) make a decision on whether it thinks the image is a morph and 2) provide a confidence score on its decision.

  To assess morph detection performance, two primary quantities are reported - the Attack Presentation Classification Error Rate (APCER) or morph miss rate and the Bona Fide Classification Error Rate (BPCER) or false detection rate (see Section 3). APCER and BPCER are reported both individually and as a tradeoff in DET analysis in this report. For the four algorithms submitted to this track, morph miss rates are generally very high (above 0.88) at a false detection rate of 0.01. This can be interpreted as ”at the cost of incorrectly claiming that 1 in every 100 legitimate photo is a morph, the percentage of actual morphs that are not being correctly detected is above 88%”. This is observed across all algorithms and all datasets tested, and is indicative of the technology maturity still being in its infancy for practical application. Large reductions in morph miss rates are observed when the false detection rate is relaxed to 0.1. *Section 4.2, 4.4*

  Caveat: There is an exception to the generally high morph miss rates observed, which is the University of Bologna's algorithm (unibo-000) results against morphs created using techniques developed also by the University of Bologna in the UNIBO Automatic Morphed Face Generation Tool v1.0 dataset. That particular dataset was generated using a set of sequestered source images and morphed using software that implemented techniques published in [4]. The unibo-000 algorithm's morph miss rate is 0.05 at a false detection rate of 0.01 on this dataset. While such results need to be caveated, it highlights an interesting data point which quantifies that morph detection software can be trained/designed to detect images created using a particular morphing process. *Section 4.2.2*

Printing and Scanning: The process of printing and scanning (printing a digital image onto paper, then scanning it back in) or re-digitalization is known to be one of the biggest challenges to morph detection. The process of printing and scanning photos is followed by a number of identity credential issuance entities (e.g. passports) worldwide in countries that rely on mail-in applications. Therefore, the use case of morph detection on printed and scanned photos is very relevant. We investigate the performance of algorithms on print and scanned photos using a subset of images (both morphs and nonmorphs) from the UNIBO Automatic Morphed Face Generation Tool v1.0 dataset, printed with an HiTi P310W photo printer, and scanned back in with a Fujitsu fi-7280 scanner at 300 PPI. For a majority of the algorithms (hdalbp-005, hdaprnu-002, ntnussl-001), morph miss rates are extremely low BUT false detection rates are extremely high, so the algorithms appear to be classifying most scanned photos as morphs, even when they're not. The unibo-000 algorithm results show that on the same set of morphed images that it was able to successfully detect originally as digital photos, once printed and scanned back in, morph miss rates increased by 49%. *Section 4.2.3*

Subject Alpha: Assuming a two-person morph, the amount that each subject contributes to the morph (i.e. subject alpha) can be varied, for example, if subject A contributes 20% then subject B would contribute 80%. For the single-image morph detection algorithms, it is observed that morph detection confidence scores are generally higher in morphs where the alpha difference is small between the subjects (e.g. 50%-50%, 40%-60%), but confidence scores are lower in morphs where the alpha difference is large between subjects (e.g. 10%-90%). This means that the algorithms are having difficulty detecting morphs that contain only small amounts of one of the subjects (and a significant amount of the other). This trend is observed for all of the single-image morph detection algorithms, in varying degrees depending on the algorithm and dataset but does not appear to exist in the two-image differential morph detection algorithm. *Section 4.6*

- **Two-image Differential Morph Detection:** In this use case, two face photos are provided to the algorithm, the first being a suspected morph and the second image representing a known, non-morphed face image of one of the subjects contributing to the morph (e.g., live capture image from an eGate). The software has to 1) make a decision on whether it thinks the image is a morph and 2) provide a confidence score on its decision. This procedure supports measurement of whether algorithms can detect morphed images when additional information (the second photo) is provided. One algorithm has been submitted to this track thus far and has been evaluated on six out of twelve datasets. Morph miss rates are at 100% at a false detection rate of 0.01 and well above 80% even at false detection rate of 0.1. In comparison, some of the single-image morph detection algorithms achieve much lower morph miss rates at both false detection thresholds on the same exact set of data (without the additional second photo). More investigation will be conducted for this track, including on the remaining datasets available for testing. *Section 4.3*

Future Work

FRVT MORPH will run continuously, and this report will be updated as new algorithms, datasets, analyses, and metrics are added.

Acknowledgements

The authors would like to thank the U.S. Department of State, Federal Bureau of Investigation, Noblis, MITRE, Otto von Guericke University of Magdeburg, University of Bologna, and the Australian Defence Science and Technology Group for their collaboration and contributions to this activity. Additionally, the authors are grateful to Hochschule Darmstadt University of Applied Sciences for discussions on test methodology and metrics.

The authors are grateful to Wayne Salamon and Greg Fiumara at NIST for designing robust software infrastructure for image storage and parallel execution of algorithms across our computers. Thanks also to Brian Cochran at NIST for providing highly available computers and network-attached storage.

Disclaimer

Specific hardware and software products identified in this report were used in order to perform the evaluations described in this document. In no case does identification of any commercial product, trade name, or vendor, imply recommendation or endorsement by the National Institute of Standards and Technology, nor does it imply that the products and equipment identified are necessarily the best available for the purpose.

The data, protocols, and metrics employed in this evaluation were chosen to support morph detection research and should not be construed as indicating how well these systems would perform in applications. While changes in the data domain, or changes in the amount of data used to build a system, can greatly influence system performance, changing the task protocols could reveal different performance strengths and weaknesses for these same systems.

Institutional Review Board

The National Institute of Standards and Technology Human Subjects Protection Office reviewed the protocol for this project and determined it is not human subjects research as defined in Department of Commerce Regulations, 15 CFR 27, also known as the Common Rule for the Protection of Human Subjects (45 CFR 46, Subpart A).

Contents

List of Figures

List of Tables

1 The FRVT MORPH Activity

Face morphing and the ability to detect it is an area of high interest to a number of photo-credential issuance agencies and those employing face recognition for identity verification. Face morphing is an image manipulation technique where two or more subjects' faces are morphed or blended together to form a single face in a photograph. Morphed photos can look very realistically like all contributing subjects. If a morphed photo gets onto an identity credential for example, multiple, if not all constituents of the morph, can use the same identity credential. Morphs can be used to fool both humans [1] [2] and current face recognition systems [3], such as those deployed in Automatic Border Control gates or eGates, which presents a vulnerability to current identity verification processes. Figure 1 illustrates the impact of morphed photos on current algorithms from some of the leading face recognition algorithms (labeled as A, B, C, and D) submitted to the NIST Ongoing FRVT 1:1 Verification test. The overlap between the morph and genuine match score distributions, and the significant percentage of morph comparisons that would successfully authenticate at FMR=0.001 provides the basis for research into how to detect this form of image manipulation.

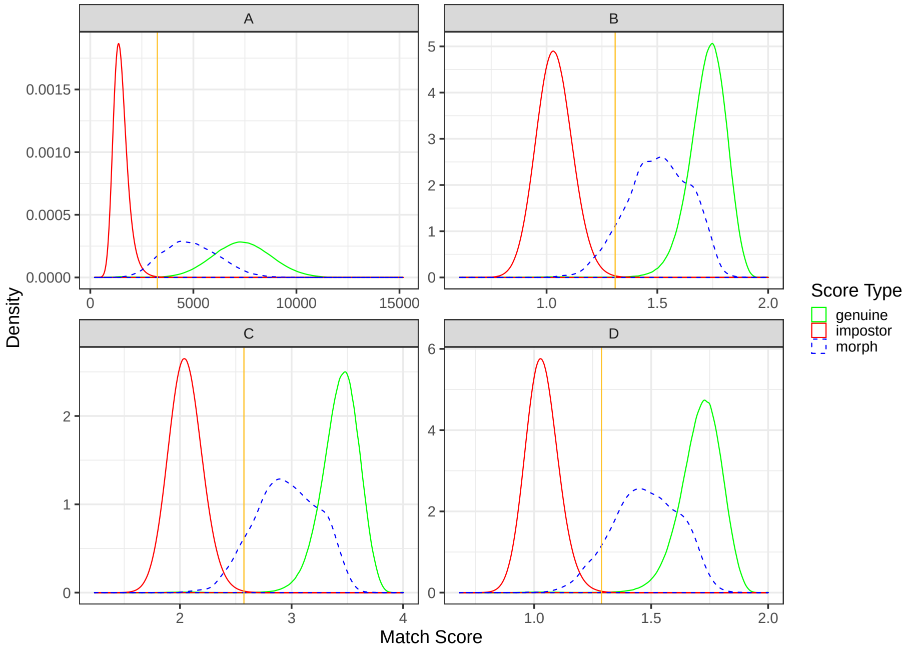

Figure 1: Morph match score distribution. The plot shows match score distribution for 1) genuine comparisons of photos of the same person (green) 2) imposter comparisons of photos of different people (red), and 3) morph comparisons of morphed photos with other photos of contributing subjects (blue). The gold line represents the score threshold at a false match rate (FMR) of 0.001. All match scores to the right of the gold line indicates that the algorithm thinks the photos are of the same person at that FMR threshold (e.g. successful authentication at an eGate).

The FRVT MORPH test will provide ongoing independent testing and measurement of prototype face morph detection technologies. The evaluation is designed to obtain an assessment of morph detection capability to inform developers and current and prospective end-users, and will evaluate two separate tasks:

- Algorithmic capability to detect face morphing (morphed/blended faces) in still photographs:
  - Single-image morph detection of non-scanned photos, printed-and-scanned photos, and images of unknown photo format/origin;
  - Two-image differential morph detection of non-scanned photos, printed-and-scanned photos, and images of unknown photo format/origin. This procedure supports measurement of whether algorithms can detect mor-

phed images when additional information, such as a live capture image, is provided.

- Face recognition algorithm resistance against morphing. The expected behavior from algorithms is to be able to correctly reject comparisons of morphed images against all constituents that contributed to the morph. The goal is to show algorithm robustness against morphing alterations when morphed images are compared against other images of the subjects used for morphing.

2 Methodology

2.1 Test Environment

The evaluation was conducted offline at a NIST facility. Offline evaluations are attractive because they allow uniform, fair, repeatable, and large-scale statistically robust testing. Testing was performed on high-end server-class blades running the CentOS Linux [5] operating system. The test harness used concurrent processing to distribute workload across dozens of computers.

2.2 Algorithms

The FRVT MORPH program is open to participation worldwide. The participation window opened in June 2018, and the test will evaluate algorithms on an ongoing basis. There is no charge to participate. The process and format of algorithm submissions to NIST are described in the FRVT MORPH Concept, Evaluation Plan, and Application Programming Interface (API) document [6]. Participants provide their submissions in the form of libraries compiled on a specified Linux kernel, which are linked against NIST's test harness to produce executables. NIST provides a validation package to participants to ensure that NIST's execution of submitted libraries produces the expected output on NIST's test machines.

This report documents the results of all algorithms submitted for testing to date. Tables 1 and 2 lists the participants who submitted algorithms to FRVT MORPH.

Participant Name	Short Name	Submission Sequence	Submission Date	Developer Notes
Hochschule Darmstadt University of Applied Sciences	hdalbp	005	2018.11.29	The idea behind the LBP implementation is based on HDA (http://dasec.h-da.de) / NTNU (https://www.ntnu.edu/nbl) approaches and published in [7–9].
Hochschule Darmstadt University of Applied Sciences	hdaprnu	002	2019.04.09	The idea behind the PRNU implementation is based on a HDA (http://dasec.h-da.de) / PLUS (http://www.wavelab.at) cooperation and published in [10,11].
Norwegian University of Science and Technology	ntnussl	001	2019.07.08	[12–14]
University of Bologna	unibo	000	2019.07.29	

Table 1: FRVT MORPH Participants (Single-image Morph Detection)

Participant Name	Short Name	Submission Sequence	Submission Date	Developer Notes
Hochschule Darmstadt University of Applied Sciences	hdawl	000	2019.03.29	

Table 2: FRVT MORPH Participants (Two-image Differential Morph Detection)

2.3 Image Datasets

Testing was performed over a number of datasets created using various methods with goals to evaluate algorithm performance over a large spectrum of morphing techniques. Testing was conducted using a tiered approach, where algorithms were evaluated on

- **Tier 1:** Lower quality morphs created with readily accessible tools available to non-experts, such as online tools from public websites and free mobile applications. These morphs are created using low effort processes and are generally low quality and contain large amounts of morphing artifacts that are visible to the human eye.
- **Tier 2:** Morphs generated using automated morphing methods based on academic research and best practices. Automated methods allow for generation of morphs in large quantities for testing.
- **Tier 3:** Higher quality morphs created using commercial-grade tools with manual processes. These are high quality morphs with very minimal visible morphing artifacts.

All source images used to generate the morphs in the test datasets are frontal, portrait-style photos. Dataset information is summarized in Tables 3, 4, 5, and sample imagery is provided in Figure 2. For morph detection, each image is accompanied by an associated image label describing the image format/origin, which includes non-scanned photos, printed-and-scanned photos, and photos of unknown format.

- **Non-scanned photos:** Photos are digital images known to not have been printed and scanned from paper. There are a number of operational use-cases for morph detection on such digital images.
- **Printed-and-scanned photos:** While there are existing techniques to detect manipulation of a digital image, once the image has been printed and scanned from paper, it leaves virtually no traces of the original image ever being manipulated. So the ability to detect whether a printed-and-scanned image contains a morph warrants investigation.
- **Photos of unknown format:** In some cases, the format and/or origin of the image in question is not known, so images with ”unknown” labels will also be tested.

2.3.1 Tier 1 - Low Quality Morphs

Dataset	Morphing Method	# Morphs	# Source Images	Image Size	Image Label	Notes
Online tool from website	Unknown	1183	558	300x400	NonScanned	

Table 3: Tier 1 datasets: morphs created with easily accessible, non-expert morphing software such as online tools from websites and mobile applications. All morphs are created with two subjects and subject alpha, where known, is 0.5 (i.e., each subject contributed equally to the morph). The image label represents the label that was provided to the algorithm while processing images from the particular dataset.

2.3.2 Tier 2 - Automated Morphs

Dataset	Morphing Method	# Morphs	# Source Images	Image Size	Image Label	Notes
Global Morph	Automated	1346	254	512x768	NonScanned	Entire source images are averaged after alignment and feature warping. Morphs were created using subjects of the same gender and ethnicity labels.
Local Morph	Automated	1346	254	512x768	NonScanned	Only the face area is averaged after alignment and feature warping; Subject A provides the periphery. Morphs were created using subjects of the same gender and ethnicity labels.
Local Morph Colorized Average	Automated	1346	254	512x768	NonScanned	Only the face area is averaged after alignment and feature warping. Subject A provides the periphery. Face area is adjusted to the average of Subject A's and Subject B's face color histograms. Morphs were created using subjects of the same gender and ethnicity labels.

Local Morph Colorized Match	Automated	1346	254	512x768	NonScanned	Only the face area is averaged after alignment and feature warping. Subject A provides the periphery. Face area is adjusted to match Subject A's color histogram. Morphs were created using subjects of the same gender and ethnicity labels.
Complete [15]	Automated	6376	233	900x1200, 1350x1350	NonScanned	
Splicing [15]	Automated	11966	233	900x1200, 1350x1350	NonScanned	
Combined [16]	Automated	12752	233	900x1200, 1350x1350	NonScanned	
UNIBO Automatic Morphed Face Generation Tool v1.0 [3, 4, 17]	Automated	2464	64	median: 696x928, min: 488x651, max: 788x1051	NonScanned	Morphs were created using subjects of the same gender and ethnicity labels.
DST	Automatic	171	487	1350x1350, 900x1200, 512x768	NonScanned	Subject A provides the periphery. Faces are detected using the Viola-Jones [18] algorithm. Techniques including Delaunay triangulation are used to develop warpable meshes, which are rendered using affine warping. [19] is applied to remove morphing artifacts. Morphs were created using subjects of the same gender and ethnicity labels.

Table 4: Tier 2 datasets: morphs created using various automated methods. All morphs are created with two subjects and subject alpha, where known, is 0.5 (i.e., each subject contributed equally to the morph). The image label represents the label that was provided to the algorithm while processing images from the particular dataset.

2.3.3 Tier 3 - High Quality Morphs

Dataset	Morphing Method	# Morphs	# Source Images	Image Size	Image Label	Notes
Manual	Commercial Tools	323	825	640x640, 1080x1080	NonScanned	
Print + Scanned		61	64	600x600	Scanned	Morphs were created using the UNIBO Automatic Morphed Face Generation Tool v1.0, then printed using an HiTi 310W photo printer and scanned back in with a Fujitsu fi-7280 scanner @ 300 PPI.

Table 5: Tier 3 datasets: morphs created using manual methods with commercial tools. All morphs are created with two subjects and subject alpha, where known, is 0.5 (i.e., each subject contributed equally to the morph). The image label represents the label that was provided to the algorithm while processing images from the particular dataset.

2.3.4 Other Datasets

Dataset	Morphing Method	# Morphs	# Source Images	Image Size	Image Label	Notes
Mugshots	-	-	1047389	499x588, 768x960, 800x1000, 1000x1330	NonScanned	

Table 6: Other datasets: additional bona fide images used to evaluate morph false detection rate.

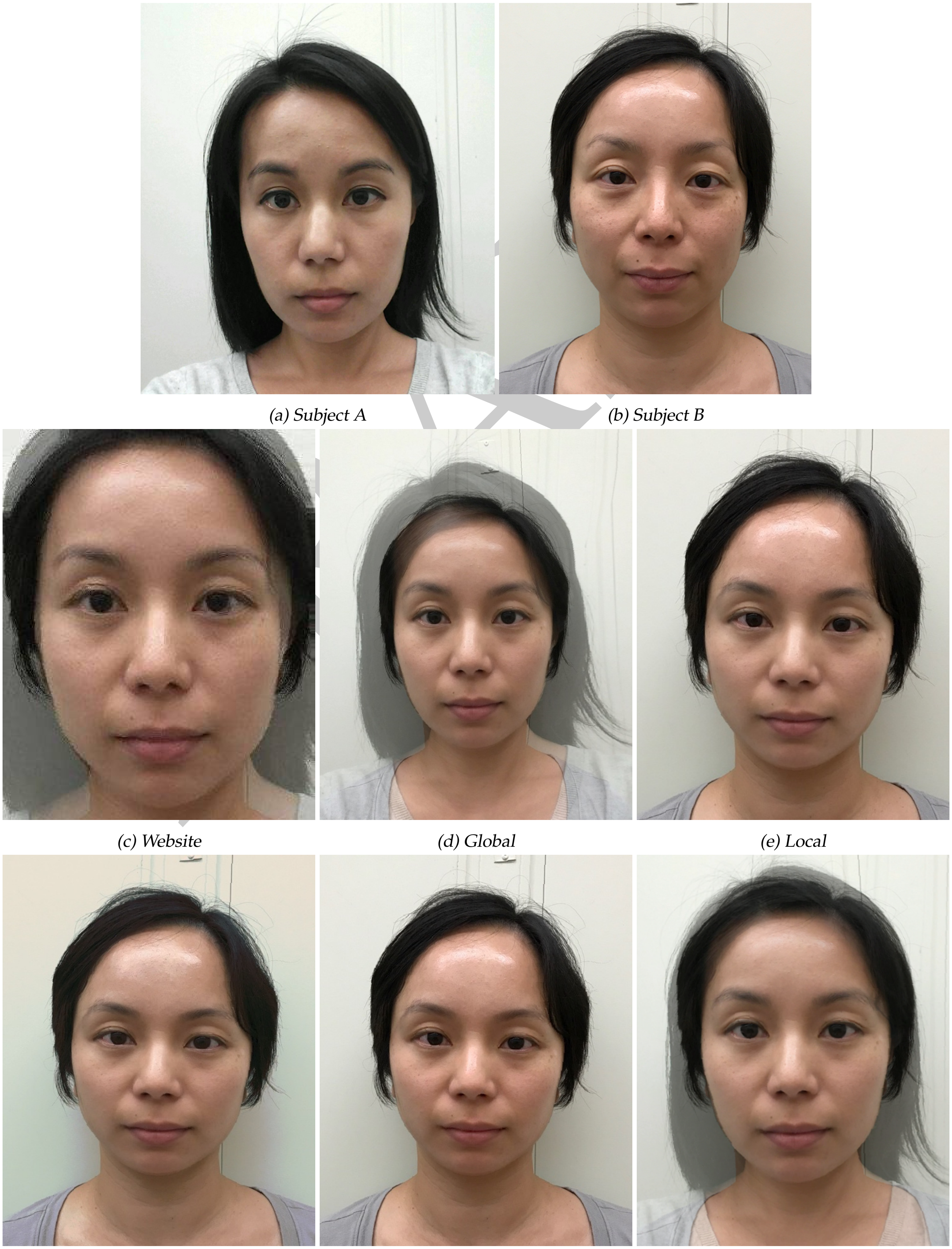

(a) Subject A

(b) Subject B

(c) Website

(d) Global

(e) Local

(f) Local Morph Colorized Average

(g) Local Morph Colorized Match

(h) Complete

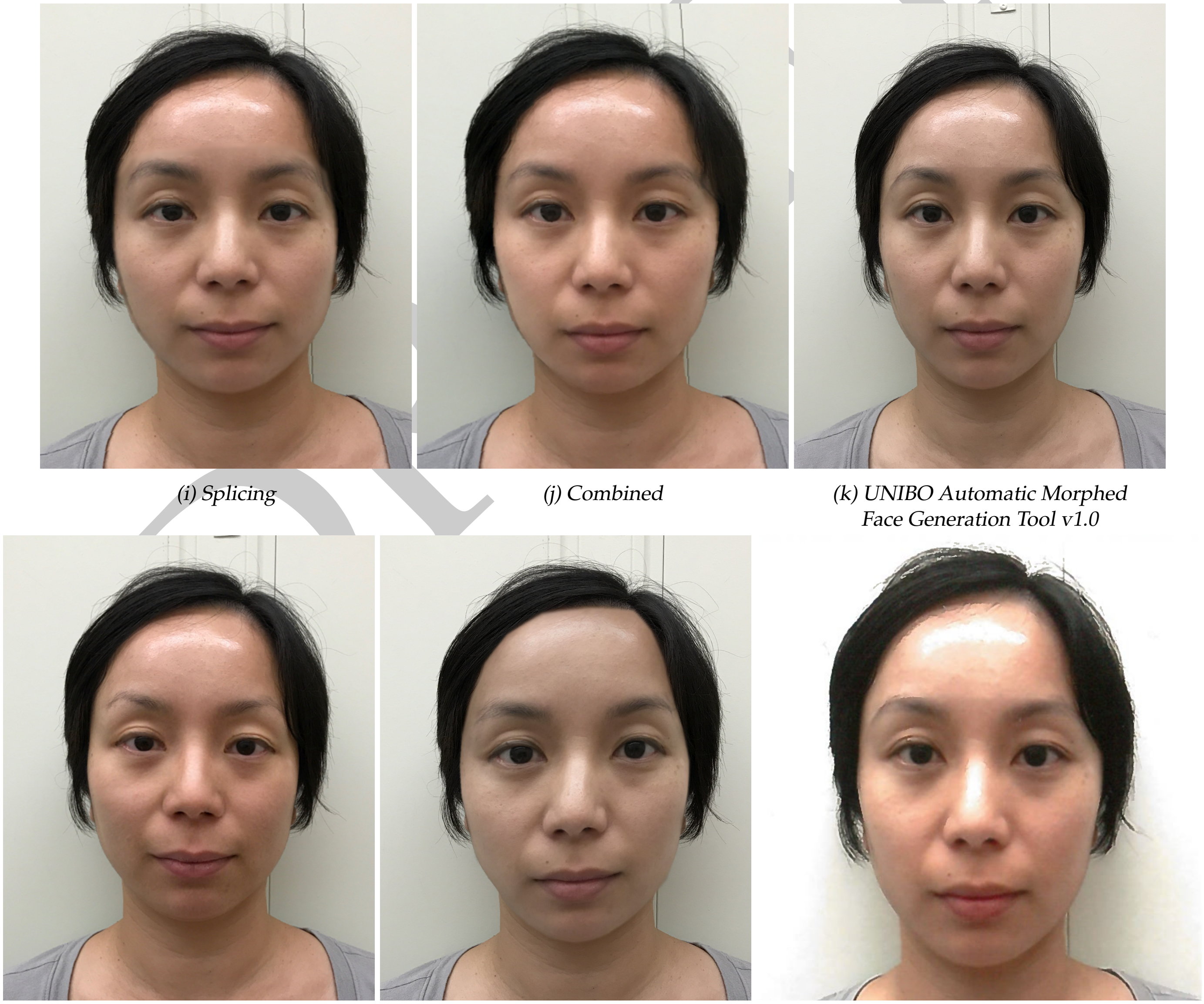

(i) Splicing

(j) Combined

(k) UNIBO Automatic Morphed Face Generation Tool v1.0

(l) DST

(m) Manual

(n) Print and Scanned

Figure 2: Samples of morphed imagery used in this report. Both subjects of the morphs are NIST employees.

3 Metrics

In this section, we adopt terminology from the presentation attack detection testing standard [20] to quantify morph classification accuracy. Morph detection or attack presentation classification requires submitted algorithms to determine whether a particular image is a morph or not. Given an image, algorithms reported a 1) binary decision on whether the image is a morph or not and 2) a confidence score on $[0, 1]$ representing the algorithm's certainty about whether the image is a morph.

3.1 Attack Presentation Classification Error Rate (APCER)

Using the algorithm's binary decision, APCER is defined as the proportion of morph attack samples incorrectly classified as bona fide (nonmorph) presentation. This is measured as the number of incorrectly classified morphed images, M, divided by the total number of morphed images, N_m. In the case of algorithm failure to process an image (i.e., the software returns a non-successful return code), those failures are not used in the calculation of APCER. The percentage of morphs that the algorithm ”failed to process” is documented as a standalone quantity in this report.

$$\text{APCER} = \frac{M}{N_m} \tag{1}$$

Note that the algorithm's binary decision is based off of some developer-defined internal threshold.

3.2 Bona Fide Presentation Classification Error Rate (BPCER)

Similarly, BPCER is defined as the proportion of bona fide (nonmorph) samples incorrectly classified as morphed samples. This is measured as the number of incorrectly classified bona fide images, B, divided by the total number of bona fide images, N_b. In the case of algorithm failure to process an image (i.e., the software returns a non-successful return code), those failures are not used in the calculation of BPCER. The percentage of bona fides that the algorithm ”failed to process” are documented as a standalone quantity in this report.

$$\text{BPCER} = \frac{B}{N_b} \tag{2}$$

3.3 Detection Error Tradeoff (DET)

We assess detection accuracy by analyzing the confidence score returned by the algorithm. In this case, the higher the confidence value, the more likely the algorithm thinks it is a morph. A reasonable approach to the detection problem is to classify an image as either a morph or bona fide image by thresholding on its confidence value.

Given N detection scores on bona fide images, b, the BPCER is computed as the proportion above some threshold, T. Similarly, given M detection scores on morphed images, m, the APCER is computed as the proportion below some threshold, T. $H(x)$ is the unit step function [21], and $H(0)$ is taken to be 1.

$$\text{BPCER}(T) = \frac{1}{N}\sum_{i=1}^{N} H(b_i - T), \tag{3}$$

$$\text{APCER}(T) = 1 - \frac{1}{M}\sum_{i=1}^{M} H(m_i - T). \tag{4}$$

In an operational setting, BPCER can be interpreted as the rate of inconvenience for those with a legitimate, bona fide photo on a passport whose photo is being incorrectly detected as a morph. The consequence of such false detections is

APCER(T)	Morph Miss Rate
BPCER(T)	False Detection Rate

additional resources required to adjudicate the bona fide photo. Conversely, APCER is the rate that fraud successfully takes place when a morphed photo on a passport is incorrectly classified as a legitimate, bona fide photo (a false negative occurs).

3.3.1 BPCER vs. APCER

Operationally, it is important that morph detection technology produce very low false detection rates given the assumption that most transactions (at an eGate for example) will be on legitimate, bona fide photos. Therefore, the error rate that needs to be controlled is the BPCER, the rate at which bona fide images are falsely classified as morphs. Additional amounts of resources will be required to adjudicate such errors, which drives the need to limit false detections. But given the technology is still in its infancy and for the purposes of comparing algorithm performance, this document analyzes APCER as a function of BPCER at various thresholds and reports APCER @ BPCER=0.01, which can be interpreted as ”the rate that morphed photos are being missed at the expense of inconveniencing one out of every one hundred persons holding a bona fide, legitimate photo.”

3.3.2 APCER vs. BPCER

Additionally, it is conventional in the presentation attack detection literature [20] and in the academic literature [7, 10], to report classification performance of morph attack detection in a single figure as BPCER at a fixed APCER. For BPCER @ APCER=0.1, this can be interpreted as ”the rate of inconveniencing people holding bona fide photos at the expense of missing one out of every ten morphs”. This document reports BPCER @ APCER=0.1.

4 Results

4.1 Accuracy Summary

This section provides summary accuracy information of all submitted algorithms against the various datasets that were tested against. Note that for the results in this section, all morphs were created with two subjects only and subject alpha, where known, was 0.5 for each subject (i.e., each subject contributed equally to the morph). Further analysis on morph detection results broken out by subject alpha are in Section 4.6.

4.1.1 BPCER

For each dataset, BPCER is evaluated using two methods. The first method, BPCER$_q$, utilizes the source images (where available) that were used to create the morphed images within each dataset. This method attempts to maintain consistent quality between the bona fides and morphs within in each dataset. The second method, BPCER$_m$, employs the use of a bona fide dataset consisting of approximately 1 million live-capture mugshot photos, which enables the measurement of APCER at low (operationally relevant) BPCER.

4.1.2 Failure to Process

A failure to process occurs when the algorithm software returns a non-successful return code from the morph detection function, indicating that something went wrong while processing the image. While these failure to process events are essentially ignored in our measurement of APCER and BPCER for now, it is important to note that operationally, such failure to process events will trigger secondary processes, which may require additional resources. Failure to process rates are documented in the accuracy tables below. For each dataset, Failure to Process (Morphs) is the proportion of morphed photos the software fails on; Failure to Process (Bona Fides)$_q$ is the proportion of source images used as bona fides the software fails to process; and Failure to Process (Bona Fides)$_m$ is the proportion of mugshot photos used as bona fides the software fails to process.

4.2 Single-image Morph Detection

4.2.1 Tier 1 - Low Quality Morphs

Algorithm	Dataset	APCER*	BPCER$_q$*	BPCER$_m$*	Failure to Process (Morphs)	Failure to Process (Bona Fides)$_q$	Failure to Process (Bona Fides)$_m$	APCER @ BPCER$_m$=0.1	APCER @ BPCER$_m$=0.01
hdalbp-005	Online tool from website	0.80	0.14	0.18	0.01	0.03	0.17	0.91	1.00
hdaprnu-002	Online tool from website	0.10	0.96	0.89	0.00	0.02	0.29	0.98	1.00
ntnussl-001	Online tool from website	0.38	0.28	-	0.00	0.00	-	-	-
unibo-000	Online tool from website	0.99	0.07	0.09	0.00	0.00	0.00	0.99	1.00

4.2.2 Tier 2 - Automated Morphs

Algorithm	Dataset	APCER*	BPCER$_q$*	BPCER$_m$*	Failure to Process (Morphs)	Failure to Process (Bona Fides)$_q$	Failure to Process (Bona Fides)$_m$	APCER @ BPCER$_m$=0.1	APCER @ BPCER$_m$=0.01
hdalbp-005	Global Morph	0.21	0.32	0.18	0.11	0.09	0.17	0.37	0.89
hdalbp-005	Local Morph	0.27	0.32	0.18	0.06	0.09	0.17	0.41	0.91
hdalbp-005	Local Morph Colorized Average	0.26	0.32	0.18	0.08	0.09	0.17	0.39	0.91
hdalbp-005	Local Morph Colorized Match	0.32	0.32	0.18	0.06	0.09	0.17	0.46	0.93
hdalbp-005	Complete	0.19	0.12	0.18	0.11	0.18	0.17	0.34	0.95
hdalbp-005	Splicing	0.25	0.12	0.18	0.10	0.18	0.17	0.43	0.97
hdalbp-005	Combined	0.22	0.12	0.18	0.07	0.18	0.17	0.38	0.96
hdalbp-005	UNIBO Automatic Morphed Face Generation Tool v1.0	0.16	0.36	0.18	0.08	0.22	0.17	0.29	0.88
hdalbp-005	DST	0.82	0.23	0.18	0.10	0.13	0.17	0.92	1.00
hdaprnu-002	Global Morph	0.19	0.48	0.89	0.03	0.10	0.29	1.00	1.00
hdaprnu-002	Local Morph	0.15	0.48	0.89	0.06	0.10	0.29	1.00	1.00
hdaprnu-002	Local Morph Colorized Average	0.13	0.48	0.89	0.04	0.10	0.29	1.00	1.00
hdaprnu-002	Local Morph Colorized Match	0.30	0.48	0.89	0.05	0.10	0.29	1.00	1.00

*APCER: This is the percentage of morphs that are not detected. Lower values are better.
*BPCER: This is the percentage of bona fides that were mistaken for morphs. Lower values are better.

hdaprnu-002	Complete	0.00	0.94	0.89	0.52	0.33	0.29	0.79	1.00
hdaprnu-002	Splicing	0.01	0.94	0.89	0.61	0.33	0.29	0.45	0.88
hdaprnu-002	Combined	0.00	0.94	0.89	0.61	0.33	0.29	0.83	1.00
hdaprnu-002	UNIBO Automatic Morphed Face Generation Tool v1.0	0.00	0.88	0.89	0.00	0.22	0.29	0.66	1.00
hdaprnu-002	DST	0.09	0.66	0.89	0.40	0.21	0.29	0.99	1.00
ntnussl-001	Global Morph	0.20	0.39	-	0.00	0.00	-	-	-
ntnussl-001	Local Morph	0.25	0.39	-	0.00	0.00	-	-	-
ntnussl-001	Local Morph Colorized Average	0.25	0.39	-	0.00	0.00	-	-	-
ntnussl-001	Local Morph Colorized Match	0.32	0.39	-	0.03	0.00	-	-	-
ntnussl-001	Complete	0.01	0.75	-	0.00	0.00	-	-	-
ntnussl-001	Splicing	0.05	0.75	-	0.00	0.00	-	-	-
ntnussl-001	Combined	0.01	0.75	-	0.00	0.00	-	-	-
ntnussl-001	UNIBO Automatic Morphed Face Generation Tool v1.0	0.02	0.78	-	0.00	0.00	-	-	-
ntnussl-001	DST	0.20	0.56	-	0.00	0.00	-	-	-
unibo-000	Global Morph	0.80	0.01	0.09	0.00	0.00	0.00	0.76	1.00
unibo-000	Local Morph	0.84	0.01	0.09	0.00	0.00	0.00	0.81	1.00
unibo-000	Local Morph Colorized Average	0.84	0.01	0.09	0.00	0.00	0.00	0.80	1.00
unibo-000	Local Morph Colorized Match	0.95	0.01	0.09	0.00	0.00	0.00	0.94	1.00
unibo-000	Complete	0.23	0.01	0.09	0.00	0.00	0.00	0.20	0.90
unibo-000	Splicing	0.33	0.01	0.09	0.00	0.00	0.00	0.30	0.91
unibo-000	Combined	0.25	0.01	0.09	0.00	0.00	0.00	0.22	0.91
unibo-000	UNIBO Automatic Morphed Face Generation Tool v1.0	0.00	0.64	0.09	0.00	0.00	0.00	0.00	0.05
unibo-000	DST	0.99	0.01	0.09	0.00	0.00	0.00	0.98	1.00

4.2.3 Tier 3 - High Quality Morphs

Algorithm	Dataset	APCER*	BPCER$_q$*	BPCER$_m$*	Failure to Process (Morphs)	Failure to Process (Bona Fides)$_q$	Failure to Process (Bona Fides)$_m$	APCER @ BPCER$_m$=0.1	APCER @ BPCER$_m$=0.01
hdalbp-005	Manual	0.84	0.28	0.18	0.24	0.36	0.17	0.90	1.00
hdalbp-005	Print + Scanned	0.08	0.76	-	0.02	0.08	-	-	-
hdaprnu-002	Manual	0.55	0.81	0.89	0.05	0.62	0.29	1.00	1.00
hdaprnu-002	Print + Scanned	0.00	1.00	-	0.00	0.06	-	-	-
ntnussl-001	Manual	0.71	0.15	-	0.00	0.02	-	-	-
ntnussl-001	Print + Scanned	0.02	0.54	-	0.00	0.02	-	-	-
unibo-000	Manual	0.98	-	0.09	0.00	-	0.00	0.97	1.00
unibo-000	Print + Scanned	0.49	0.05	-	0.00	0.02	-	-	-

4.3 Two-image Differential Morph Detection

4.3.1 Tier 1 - Low Quality Morphs

Algorithm	Dataset	APCER*	BPCER$_q$*	BPCER$_m$*	Failure to Process (Morphs)	Failure to Process (Bona Fides)$_q$	Failure to Process (Bona Fides)$_m$	APCER @ BPCER$_m$=0.1	APCER @ BPCER$_m$=0.01
hdawl-000	Online tool from website	0.25	0.73	0.79	0.61	0.63	0.36	0.90	1.00

4.3.2 Tier 2 - Automated Morphs

Algorithm	Dataset	APCER*	BPCER$_q$*	BPCER$_m$*	Failure to Process (Morphs)	Failure to Process (Bona Fides)$_q$	Failure to Process (Bona Fides)$_m$	APCER @ BPCER$_m$=0.1	APCER @ BPCER$_m$=0.01
hdawl-000	Global Morph	0.33	0.53	0.79	0.13	0.18	0.36	0.95	1.00
hdawl-000	Local Morph	0.28	0.53	0.79	0.17	0.18	0.36	0.93	1.00
hdawl-000	Local Morph Colorized Average	0.30	0.53	0.79	0.15	0.18	0.36	0.94	1.00
hdawl-000	Local Morph Colorized Match	0.27	0.53	0.79	0.16	0.18	0.36	0.94	1.00

*APCER: This is the percentage of morphs that are not detected. Lower values are better.
*BPCER: This is the percentage of bona fides that were mistaken for morphs. Lower values are better.

4.3.3 Tier 3 - High Quality Morphs

Algorithm	Dataset	APCER*	BPCER$_q{}^{\star}$	BPCER$_m{}^{\star}$	Failure to Process (Morphs)	Failure to Process (Bona Fides)$_q$	Failure to Process (Bona Fides)$_m$	APCER @ BPCER$_m$=0.1	APCER @ BPCER$_m$=0.01
hdawl-000	Manual	0.10	0.73	0.79	0.65	0.63	0.36	0.84	1.00

4.4 DET Analyses (BPCER vs. APCER)

4.4.1 Tier 1 - Low Quality Morphs

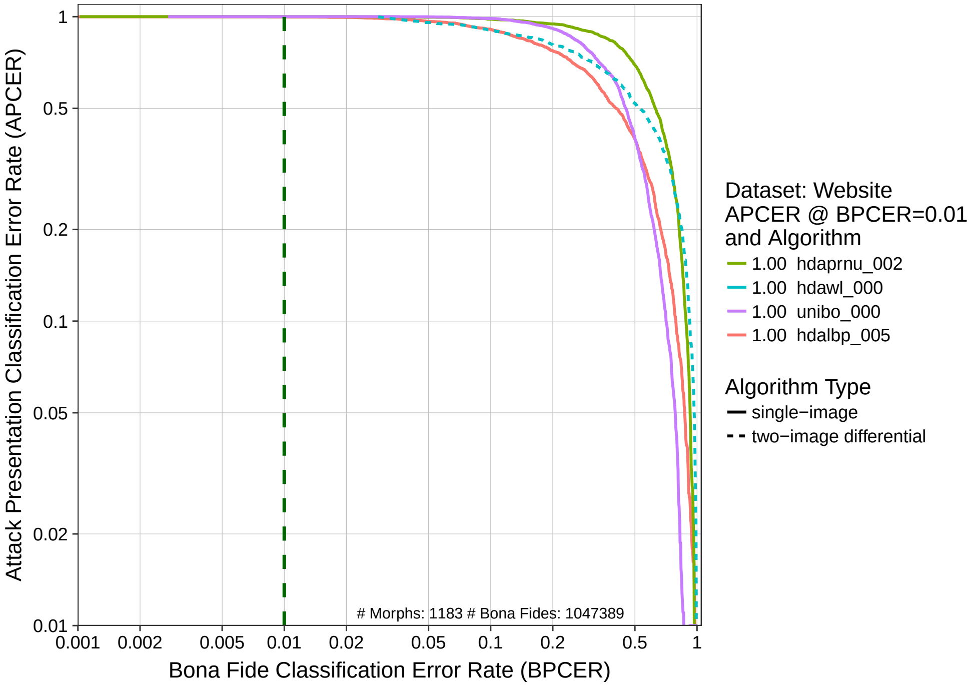

Figure 3: DET plot. This charts plots APCER as a function of BPCER. The x-axis is the rate that bona fide images are falsely classified as morphs, and the y-axis is the rate that morphs are not detected. The dotted dark green line represents BPCER=0.01.

4.4.2 Tier 2 - Automated Morphs

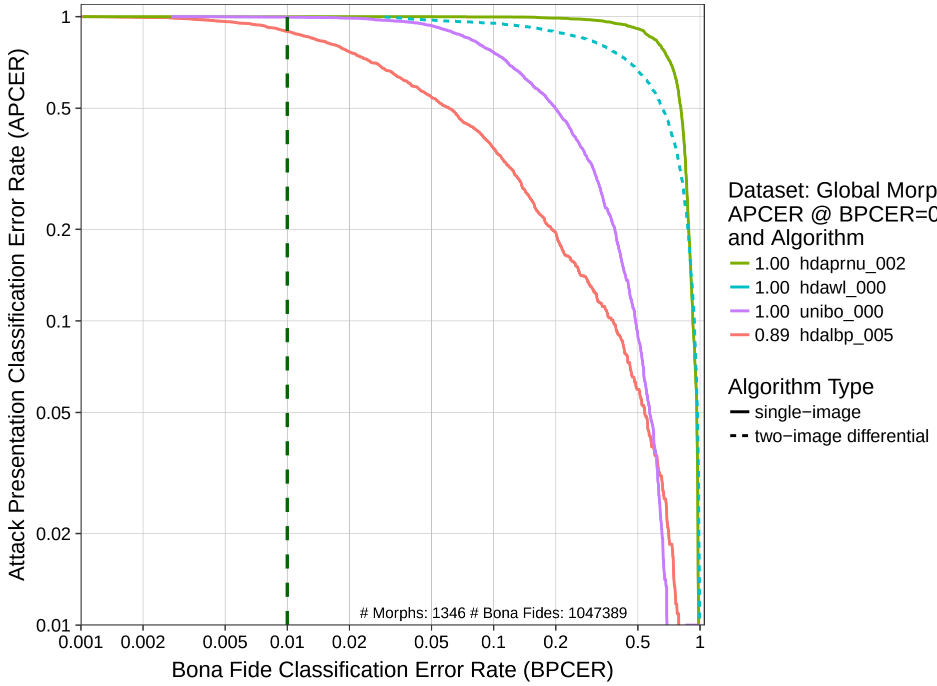

Figure 4: DET plot. This charts plots APCER as a function of BPCER. The x-axis is the rate that bona fide images are falsely classified as morphs, and the y-axis is the rate that morphs are not detected. The dotted dark green line represents BPCER=0.01.

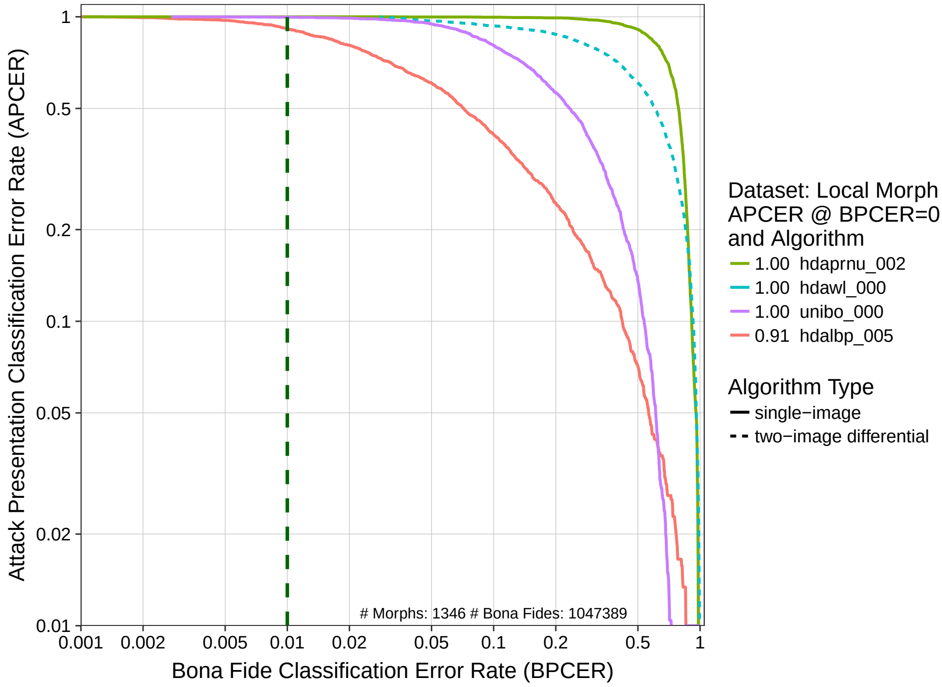

Figure 5: DET plot. This charts plots APCER as a function of BPCER. The x-axis is the rate that bona fide images are falsely classified as morphs, and the y-axis is the rate that morphs are not detected. The dotted dark green line represents BPCER=0.01.

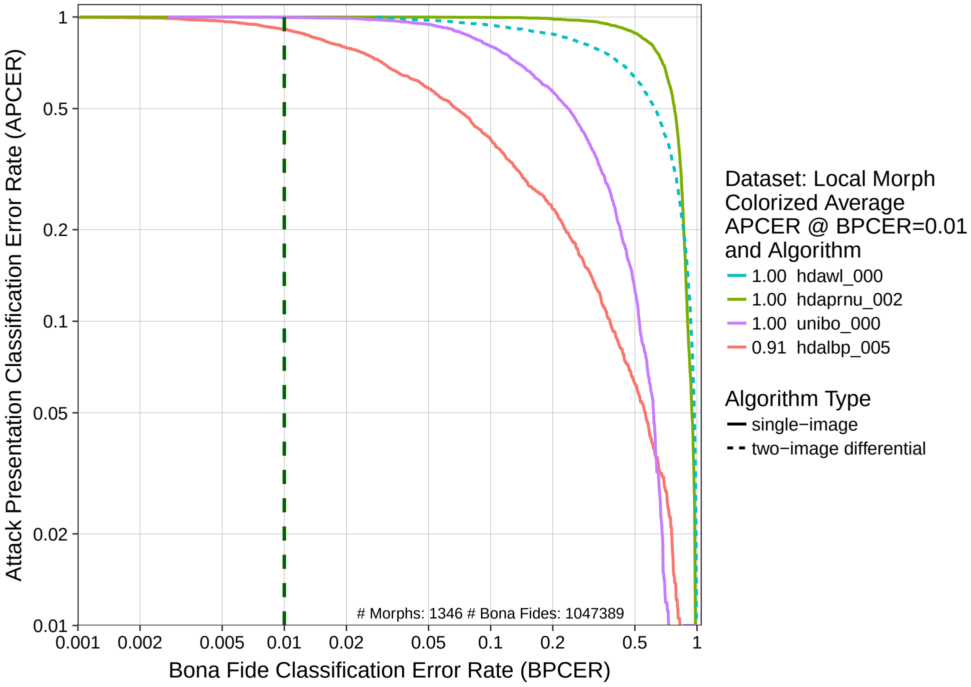

Figure 6: DET plot. This charts plots APCER as a function of BPCER. The x-axis is the rate that bona fide images are falsely classified as morphs, and the y-axis is the rate that morphs are not detected. The dotted dark green line represents BPCER=0.01.

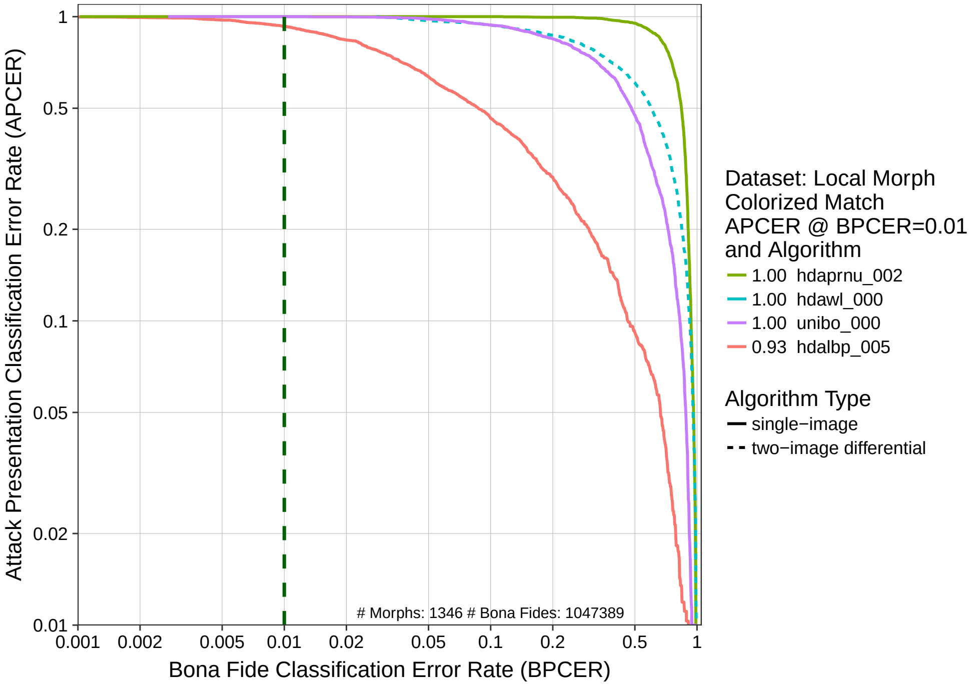

Figure 7: DET plot. This charts plots APCER as a function of BPCER. The x-axis is the rate that bona fide images are falsely classified as morphs, and the y-axis is the rate that morphs are not detected. The dotted dark green line represents BPCER=0.01.

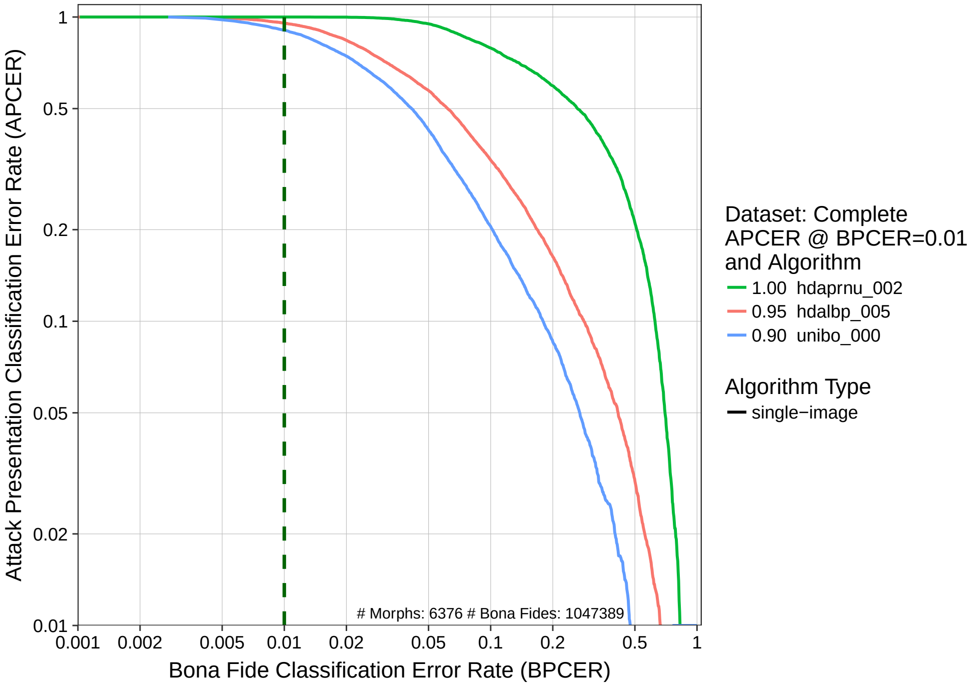

Figure 8: DET plot. This charts plots APCER as a function of BPCER. The x-axis is the rate that bona fide images are falsely classified as morphs, and the y-axis is the rate that morphs are not detected. The dotted dark green line represents BPCER=0.01.

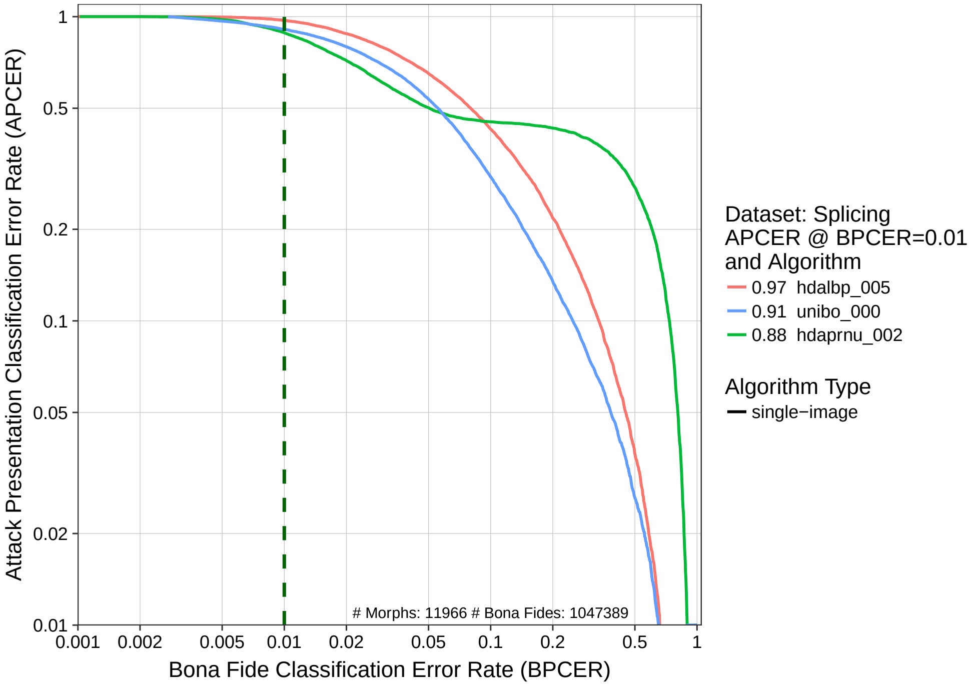

Figure 9: DET plot. This charts plots APCER as a function of BPCER. The x-axis is the rate that bona fide images are falsely classified as morphs, and the y-axis is the rate that morphs are not detected. The dotted dark green line represents BPCER=0.01.

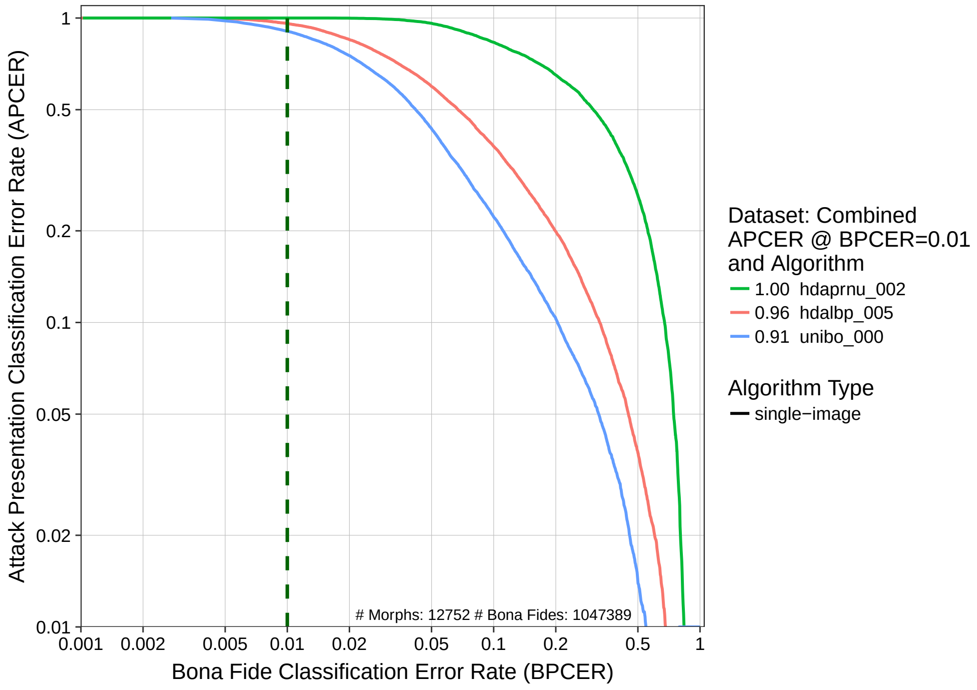

Figure 10: DET plot. This charts plots APCER as a function of BPCER. The x-axis is the rate that bona fide images are falsely classified as morphs, and the y-axis is the rate that morphs are not detected. The dotted dark green line represents BPCER=0.01.

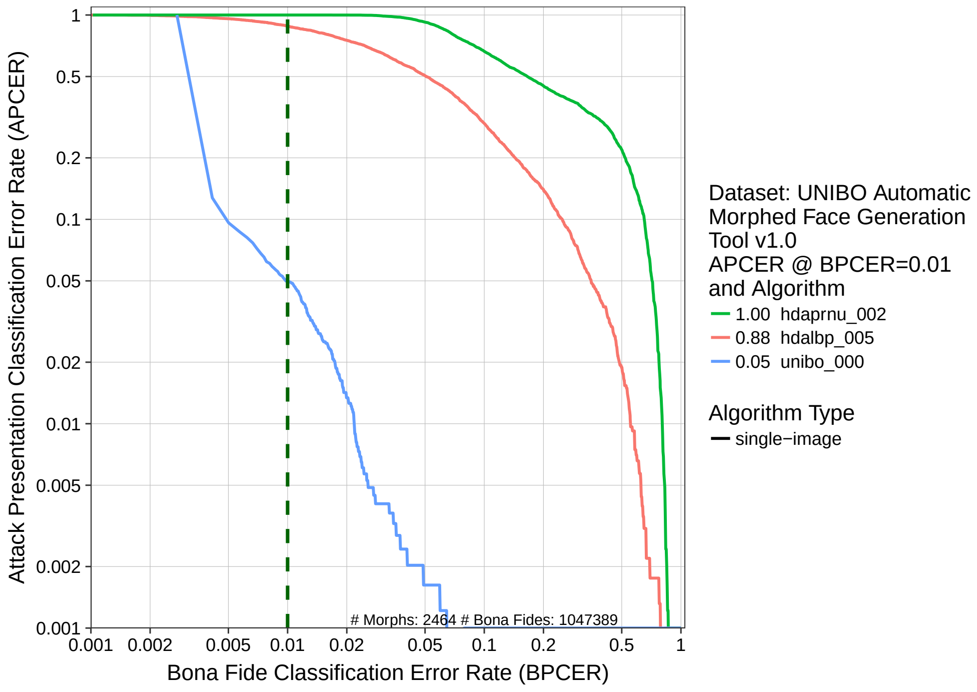

Figure 11: DET plot. This charts plots APCER as a function of BPCER. The x-axis is the rate that bona fide images are falsely classified as morphs, and the y-axis is the rate that morphs are not detected. The dotted dark green line represents BPCER=0.01.

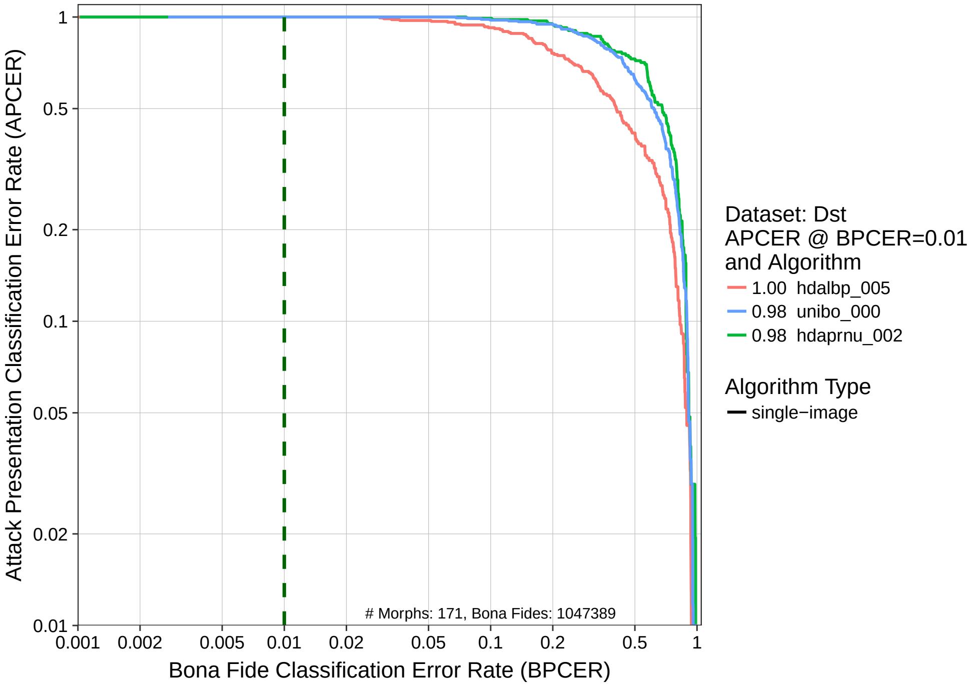

Figure 12: DET plot. This charts plots APCER as a function of BPCER. The x-axis is the rate that bona fide images are falsely classified as morphs, and the y-axis is the rate that morphs are not detected. The dotted dark green line represents BPCER=0.01.

4.4.3 Tier 3 - High Quality Morphs

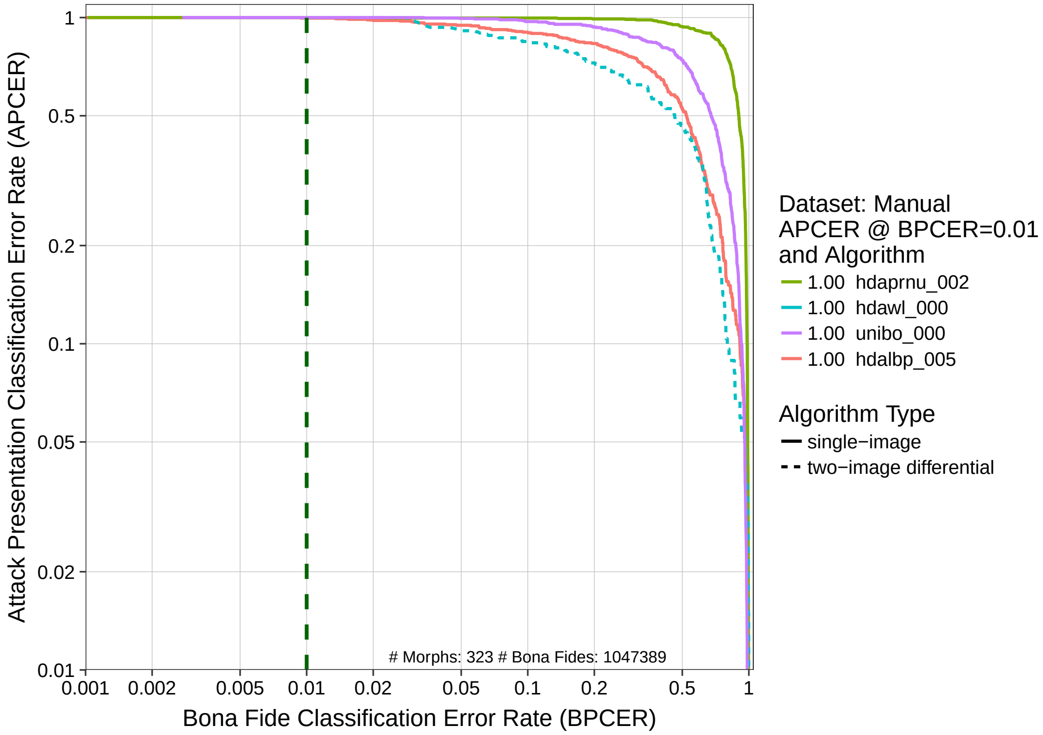

Figure 13: DET plot. This charts plots APCER as a function of BPCER. The x-axis is the rate that bona fide images are falsely classified as morphs, and the y-axis is the rate that morphs are not detected. The dotted dark green line represents BPCER=0.01.

4.5 DET Analyses (APCER vs. BPCER)

4.5.1 Tier 1 - Low Quality Morphs

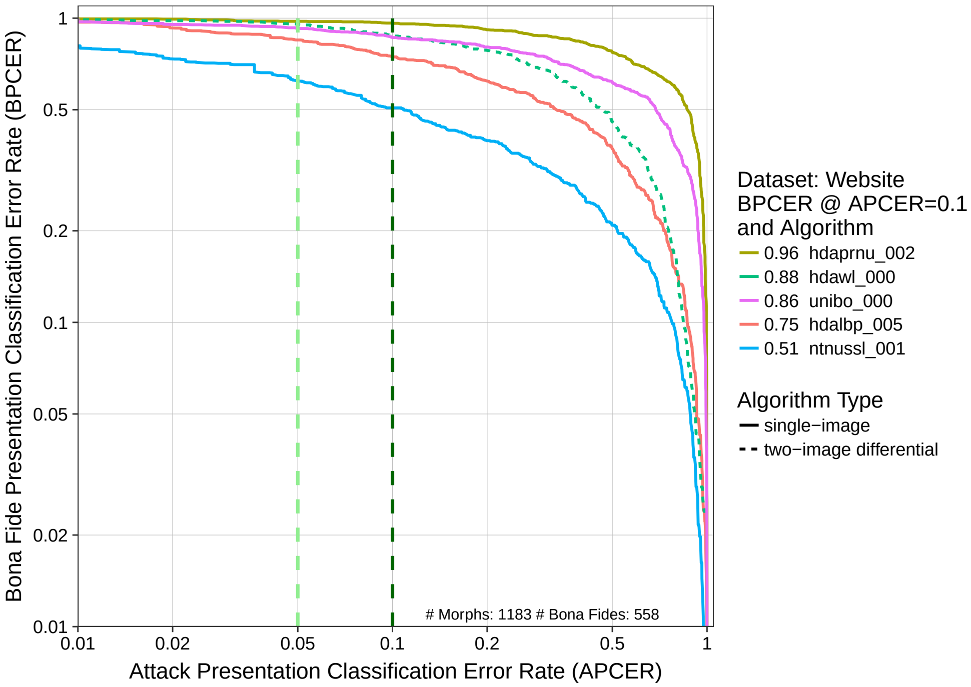

Figure 14: DET plot. This charts plots BPCER as a function of APCER. The x-axis is the rate that morphs are not detected, and the y-axis is the rate that bona fide images are falsely classified as morphs. The dotted dark green and light green lines represent APCER=0.1 and 0.05, respectively.

4.5.2 Tier 2 - Automated Morphs

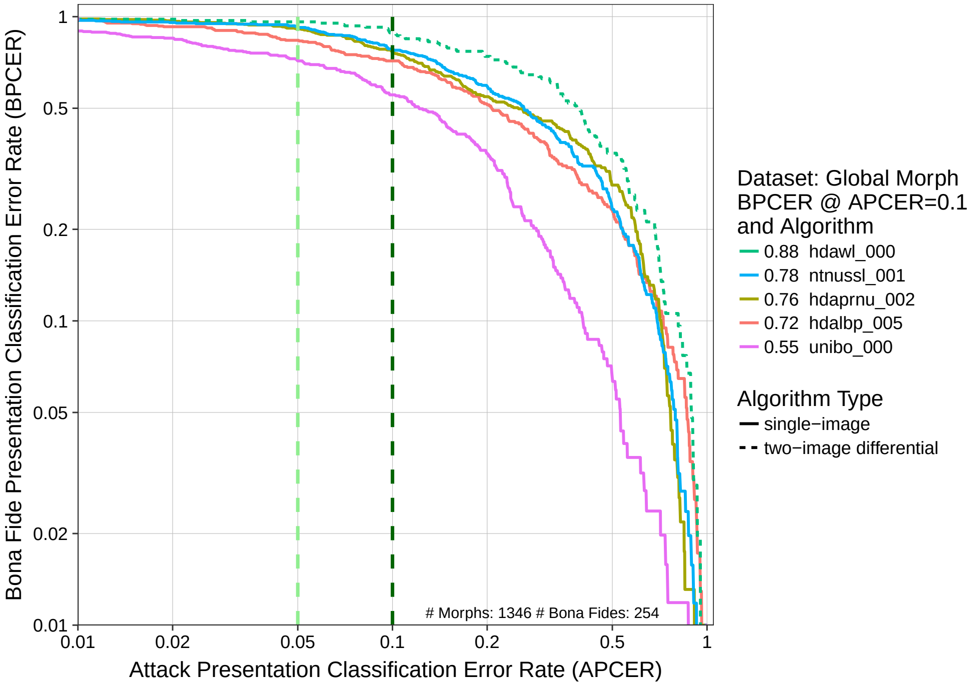

Figure 15: DET plot. This charts plots BPCER as a function of APCER. The x-axis is the rate that morphs are not detected, and the y-axis is the rate that bona fide images are falsely classified as morphs. The dotted dark green and light green lines represent APCER=0.1 and 0.05, respectively.

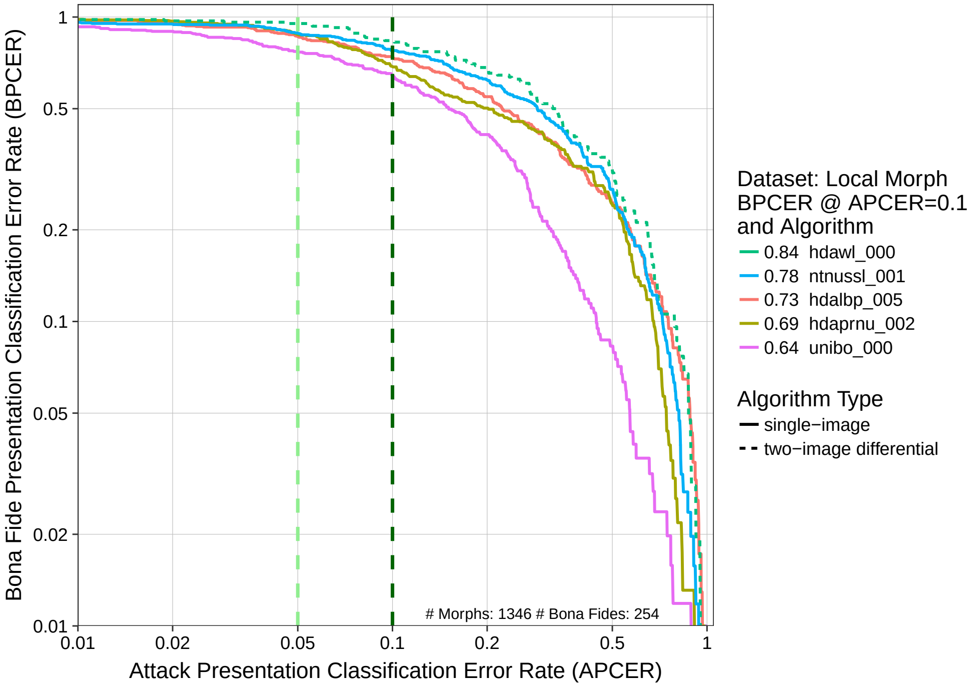

Figure 16: DET plot. This charts plots BPCER as a function of APCER. The x-axis is the rate that morphs are not detected, and the y-axis is the rate that bona fide images are falsely classified as morphs. The dotted dark green and light green lines represent APCER=0.1 and 0.05, respectively.

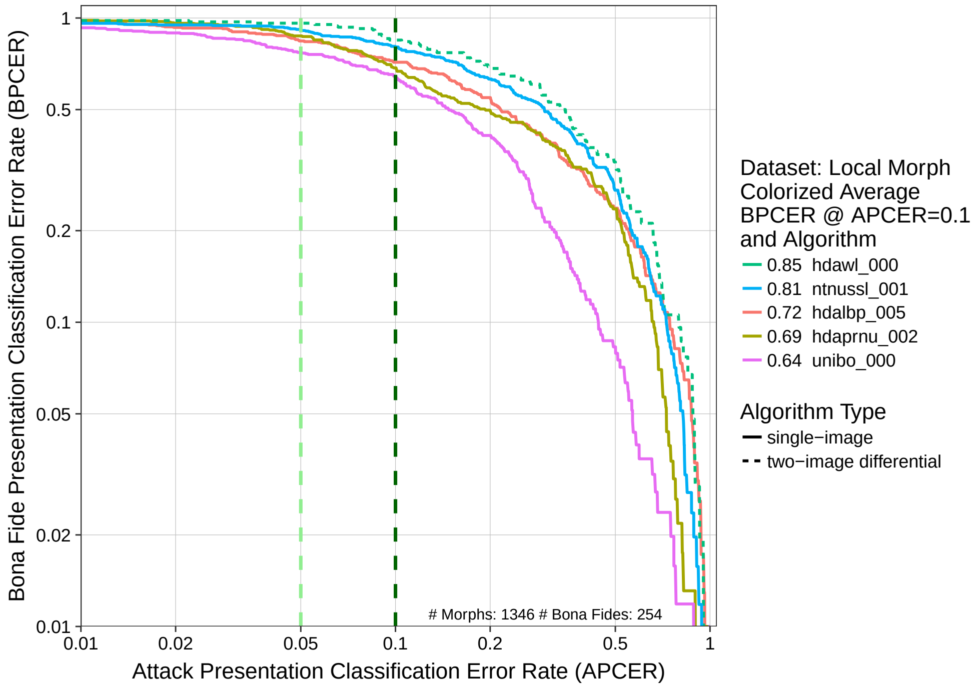

Figure 17: DET plot. This charts plots BPCER as a function of APCER. The x-axis is the rate that morphs are not detected, and the y-axis is the rate that bona fide images are falsely classified as morphs. The dotted dark green and light green lines represent APCER=0.1 and 0.05, respectively.

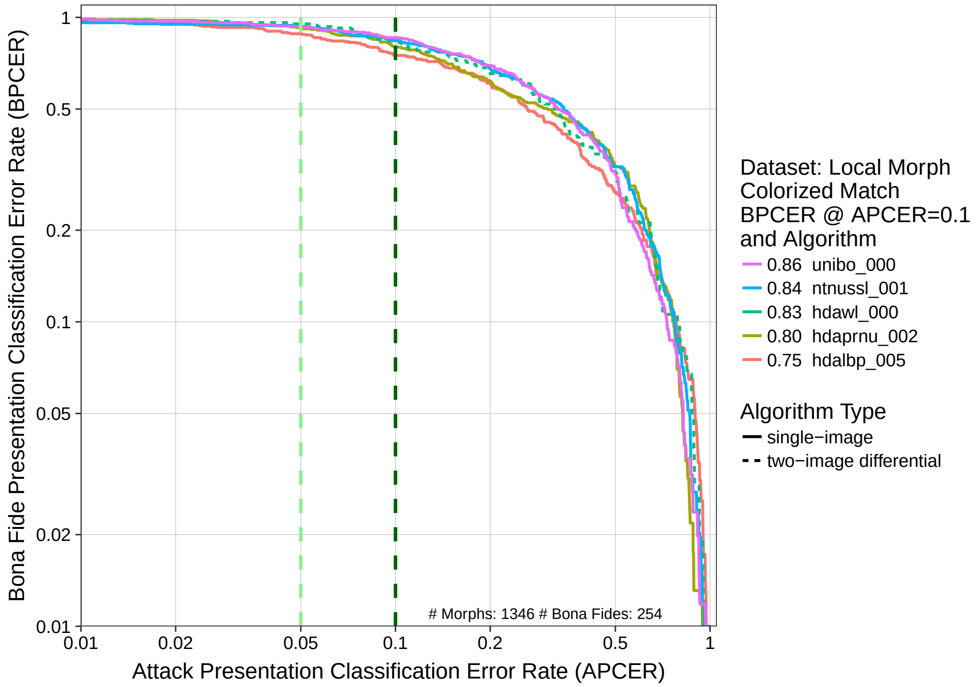

Figure 18: DET plot. This charts plots BPCER as a function of APCER. The x-axis is the rate that morphs are not detected, and the y-axis is the rate that bona fide images are falsely classified as morphs. The dotted dark green and light green lines represent APCER=0.1 and 0.05, respectively.

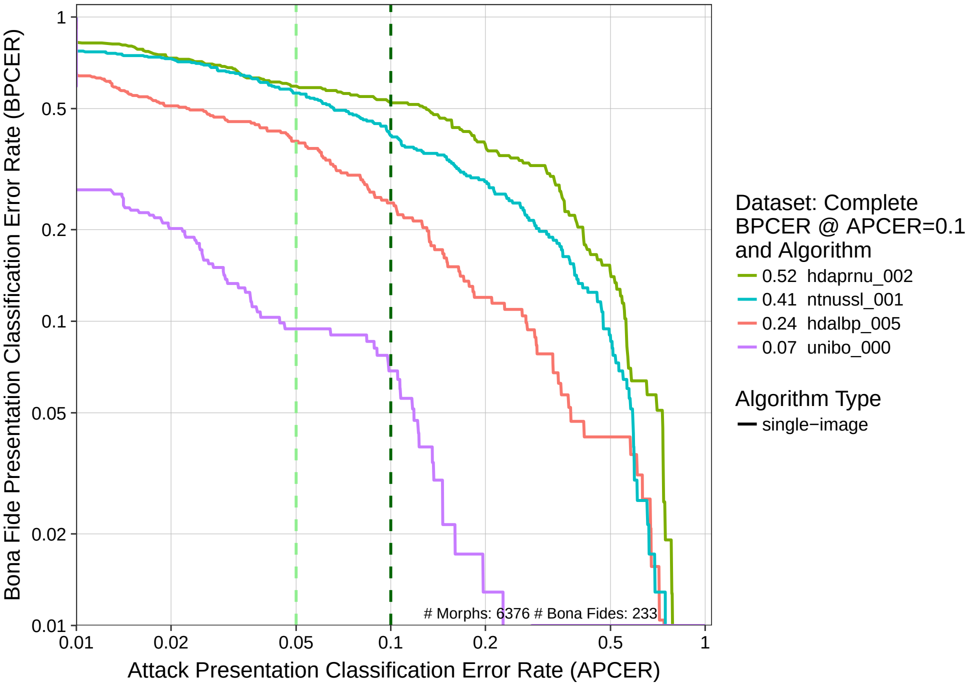

Figure 19: DET plot. This charts plots BPCER as a function of APCER. The x-axis is the rate that morphs are not detected, and the y-axis is the rate that bona fide images are falsely classified as morphs. The dotted dark green and light green lines represent APCER=0.1 and 0.05, respectively.

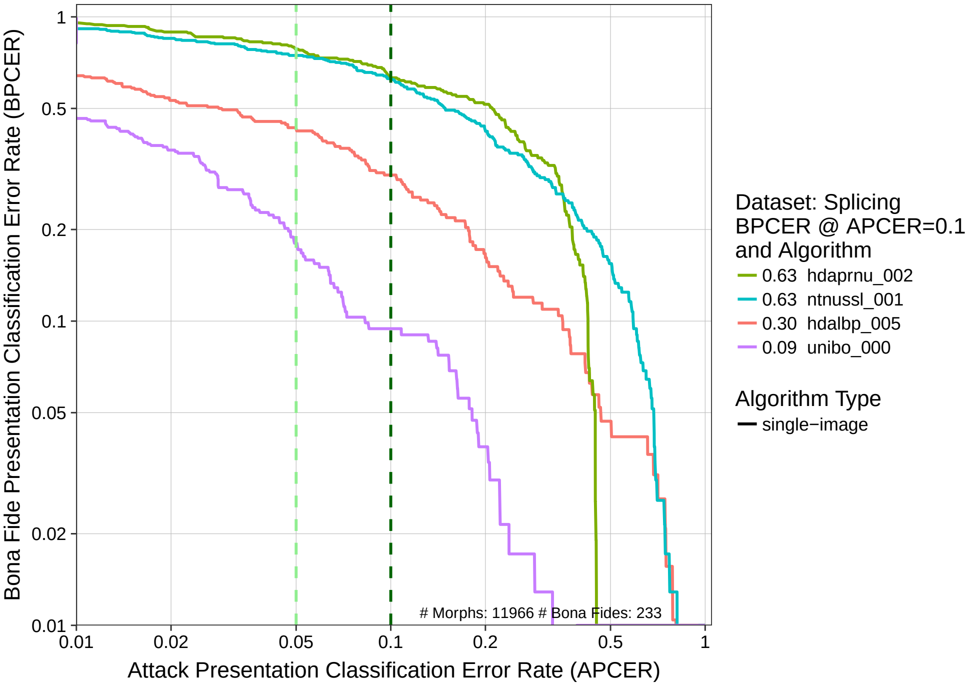

Figure 20: DET plot. This charts plots BPCER as a function of APCER. The x-axis is the rate that morphs are not detected, and the y-axis is the rate that bona fide images are falsely classified as morphs. The dotted dark green and light green lines represent APCER=0.1 and 0.05, respectively.

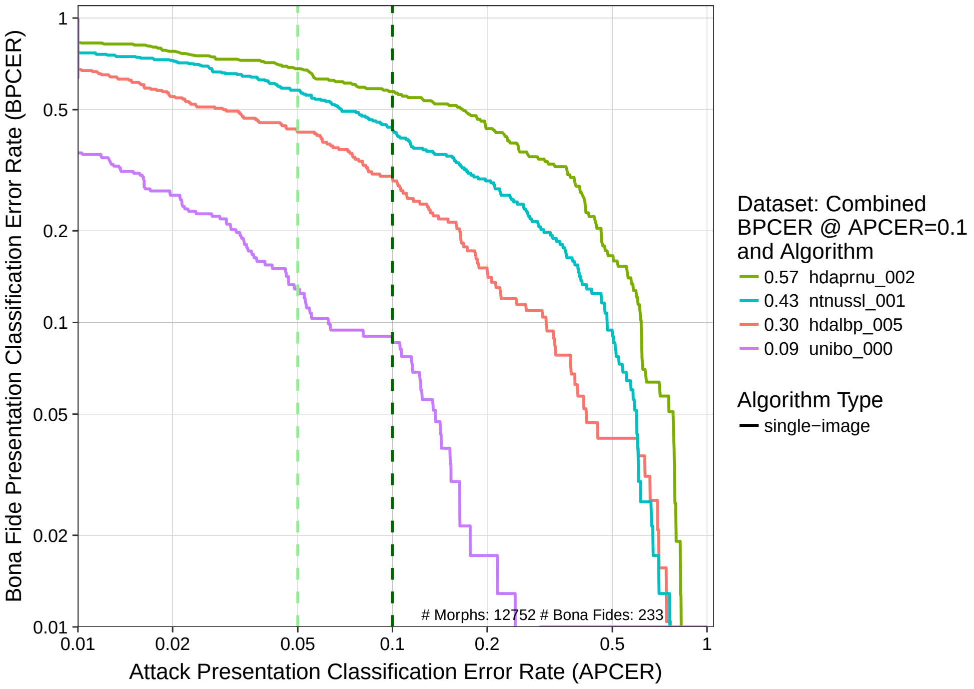

Figure 21: DET plot. This charts plots BPCER as a function of APCER. The x-axis is the rate that morphs are not detected, and the y-axis is the rate that bona fide images are falsely classified as morphs. The dotted dark green and light green lines represent APCER=0.1 and 0.05, respectively.

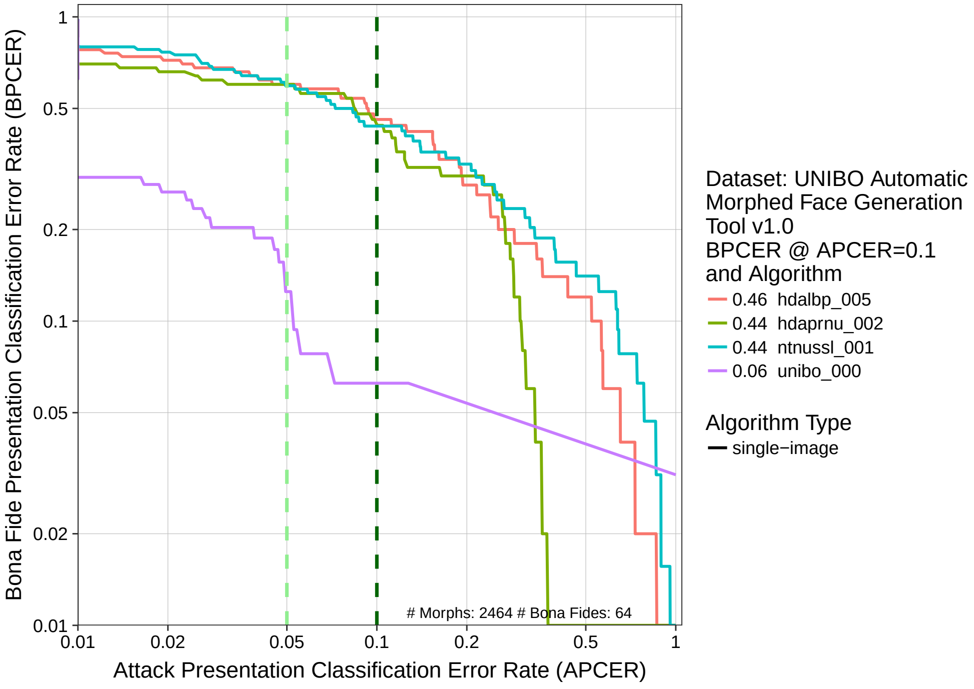

Figure 22: DET plot. This charts plots BPCER as a function of APCER. The x-axis is the rate that morphs are not detected, and the y-axis is the rate that bona fide images are falsely classified as morphs. The dotted dark green and light green lines represent APCER=0.1 and 0.05, respectively.

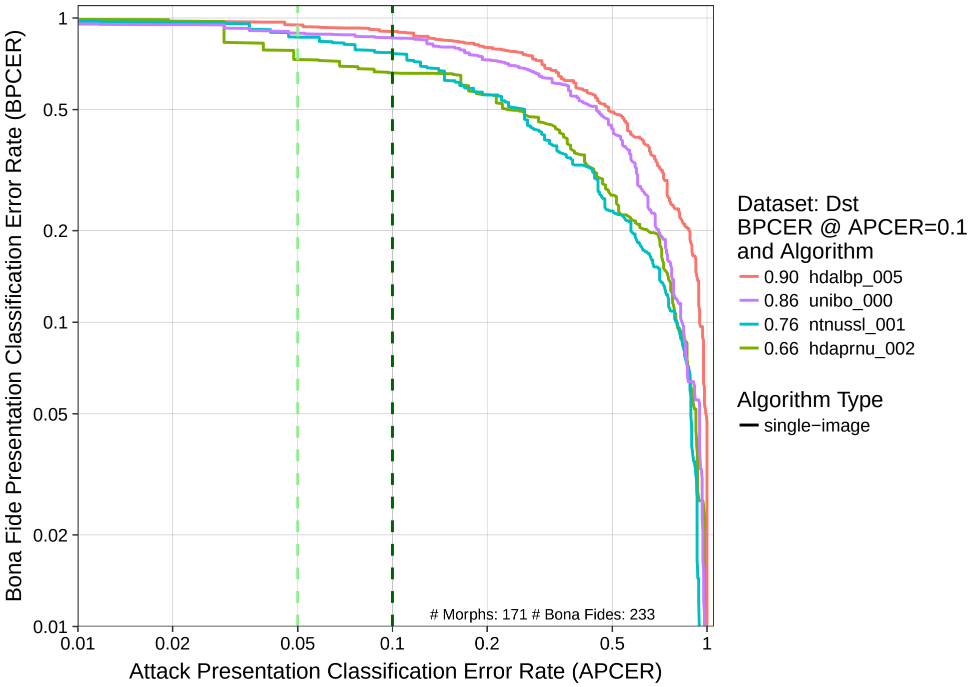

Figure 23: DET plot. This charts plots BPCER as a function of APCER. The x-axis is the rate that morphs are not detected, and the y-axis is the rate that bona fide images are falsely classified as morphs. The dotted dark green and light green lines represent APCER=0.1 and 0.05, respectively.

4.5.3 Tier 3 - High Quality Morphs

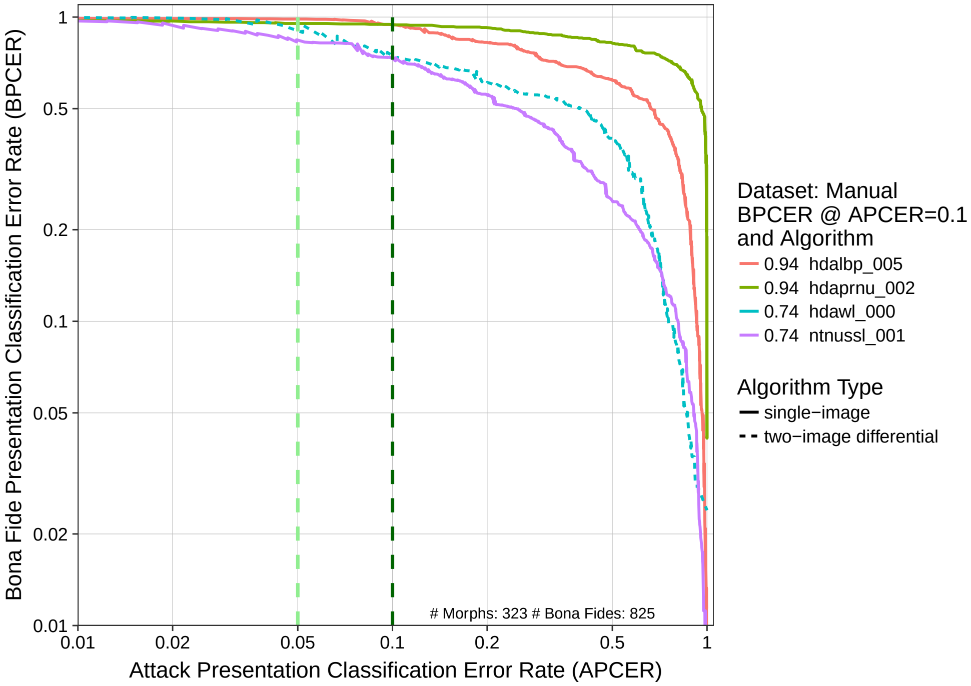

Figure 24: DET plot. This charts plots BPCER as a function of APCER. The x-axis is the rate that morphs are not detected, and the y-axis is the rate that bona fide images are falsely classified as morphs. The dotted dark green and light green lines represent APCER=0.1 and 0.05, respectively.

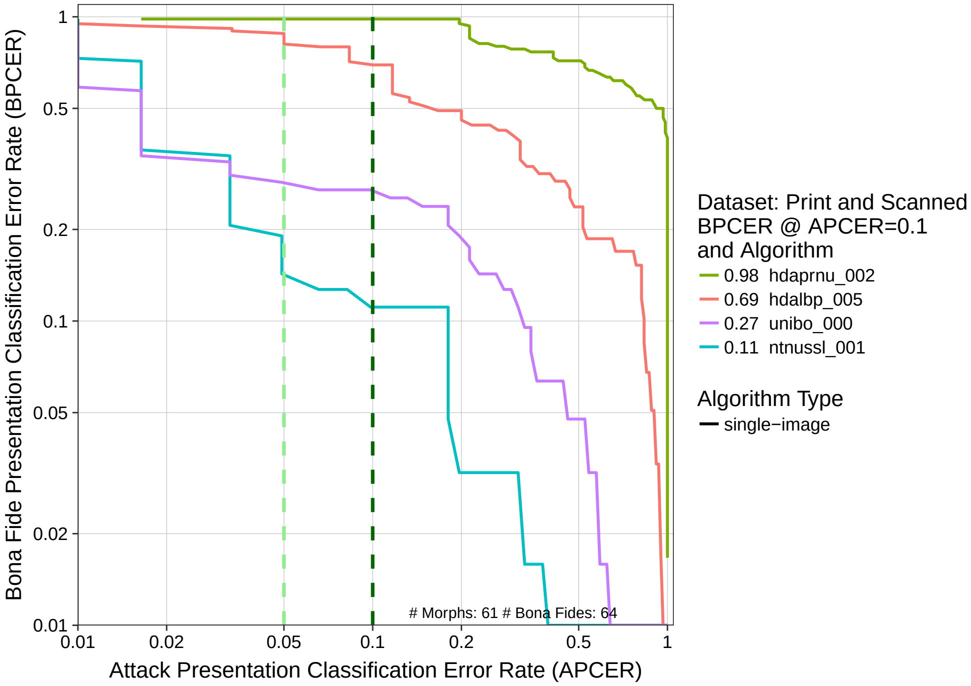

Figure 25: DET plot. This charts plots BPCER as a function of APCER. The x-axis is the rate that morphs are not detected, and the y-axis is the rate that bona fide images are falsely classified as morphs. The dotted dark green and light green lines represent APCER=0.1 and 0.05, respectively.

4.6 Impact of Subject Alpha

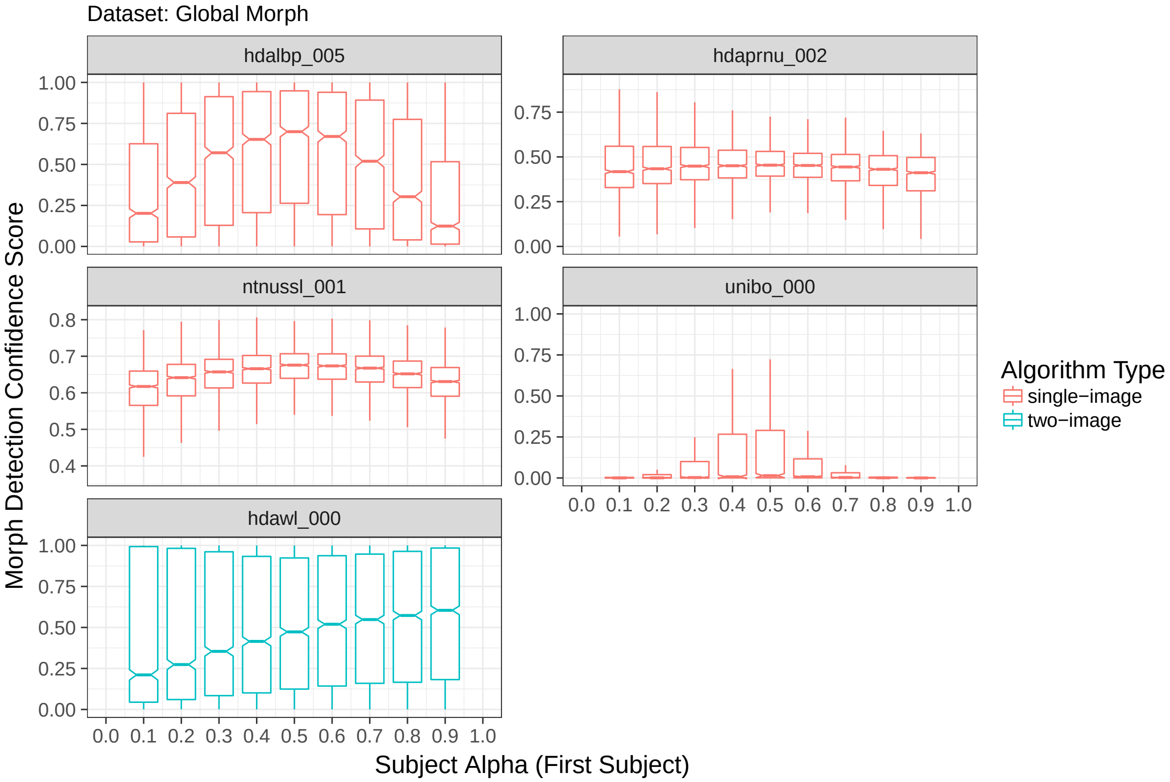

Figure 26: Boxplots plotting morph detection confidence score as a function of subject alpha (first subject in morph).

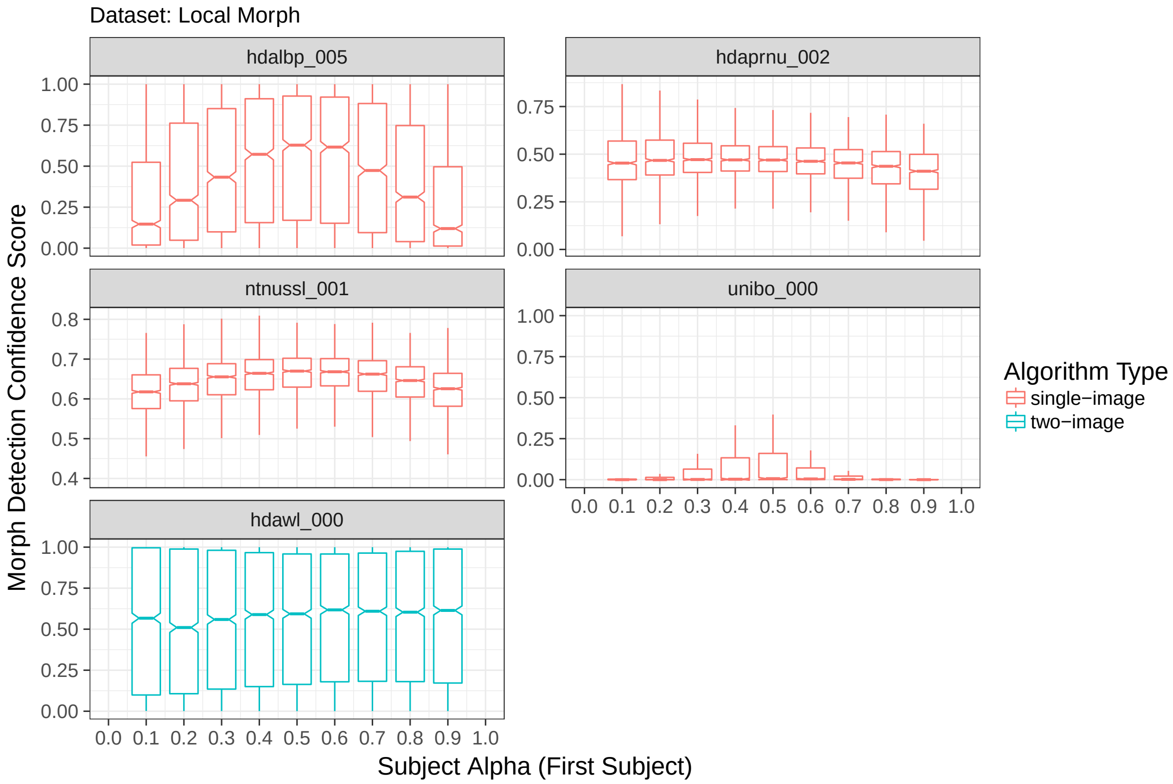

Figure 27: Boxplots plotting morph detection confidence score as a function of subject alpha (first subject in morph).

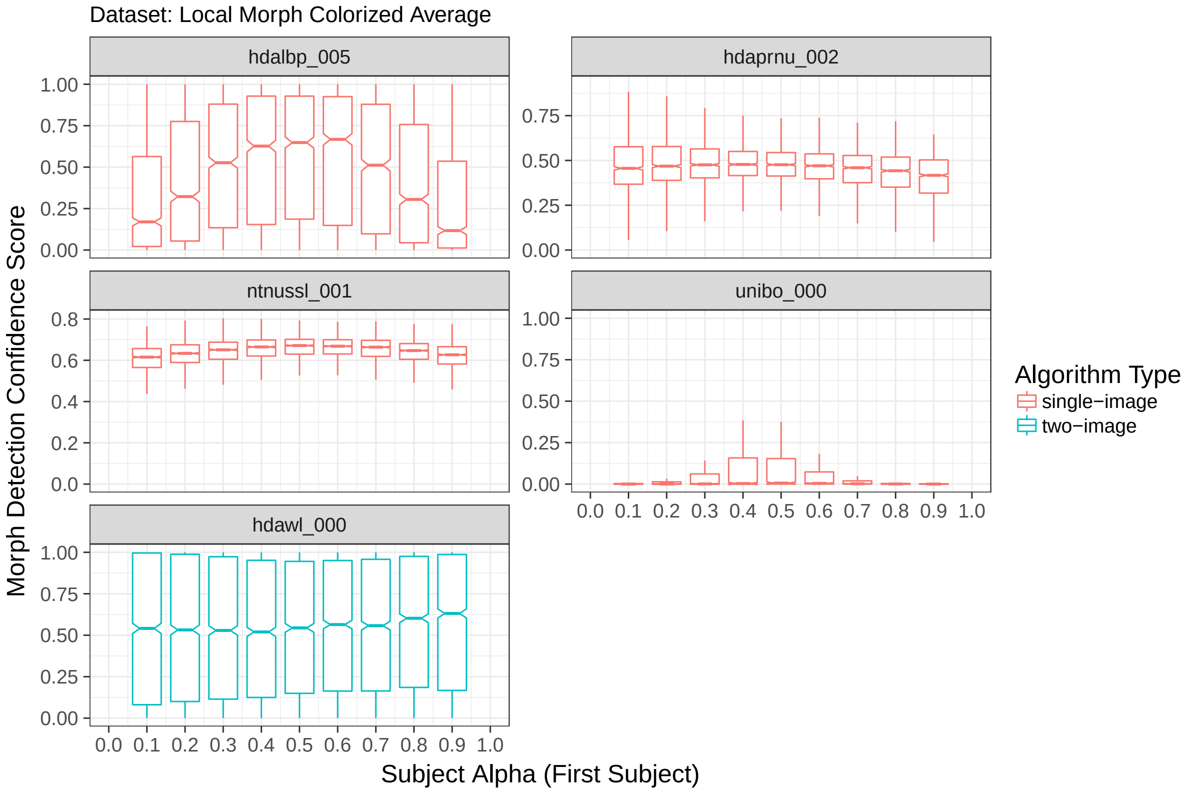

Figure 28: Boxplots plotting morph detection confidence score as a function of subject alpha (first subject in morph).

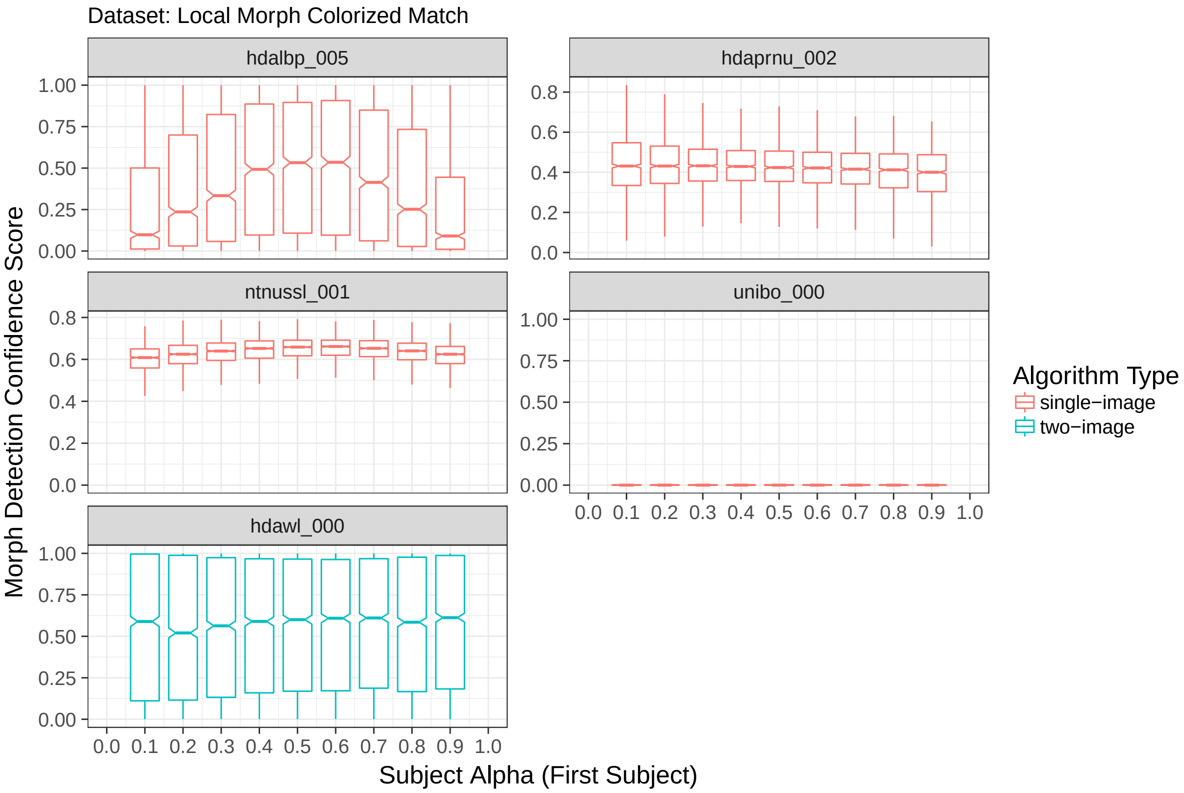

Figure 29: Boxplots plotting morph detection confidence score as a function of subject alpha (first subject in morph).

References

[1] Matteo Ferrara, Annalisa Franco, and Davide Maltoni. *On the Effects of Image Alterations on Face Recognition Accuracy*, pages 195–222. Springer International Publishing, Cham, 2016.

[2] David J. Robertson, Robin S. S. Kramer, and A. Mike Burton. Fraudulent id using face morphs: Experiments on human and automatic recognition. *PLOS ONE*, 12(3):1–12, 03 2017.

[3] M. Ferrara, A. Franco, and D. Maltoni. The magic passport. In *IEEE International Joint Conference on Biometrics*, pages 1–7, Sep. 2014.

[4] M. Ferrara, A. Franco, and D. Maltoni. Face demorphing. *IEEE Transactions on Information Forensics and Security*, 13(4):1008–1017, April 2018.

[5] The CentOS Project. https://www.centos.org.

[6] Mei Ngan, Patrick Grother, and Kayee Hanaoka. Face Recognition Vendor Test (FRVT) MORPH Concept, Evaluation Plan, and API, September 2018. https://www.nist.gov/programs-projects/face-recognition-vendor-test-frvt-morph.

[7] Ulrich Scherhag, Christian Rathgeb, and Christoph Busch. Morph detection from single face images: a multi-algorithm fusion approach. In *Proc. Int. Conf. on Biometric Engineering and Applications (ICBEA18)*, 2018.

[8] Ulrich Scherhag, Christian Rathgeb, and Christoph Busch. Towards detection of morphed face images in electronic travel documents. In *Proc. 13th IAPR Workshop on Document Analysis Systems (DAS18)*, 2018.

[9] Ulrich Scherhag, R. Ramachandra, Kiran Raja, Marta Gomez-Barrero, and Christoph Busch Christian Rathgeb. On the Vulnerability and Detection of Digital Morphed and Scanned Face Images. In *Proc. International Workshop on Biometrics and Forensics (IWBF17)*, 2017.

[10] L. Debiasi, C. Rathgeb, U. Scherhag, A. Uhl, and C. Busch. PRNU Variance Analysis for Morphed Face Image Detection. In *Proceedings of 9th International Conference on Biometrics: Theory, Applications and Systems (BTAS 2018)*, 2018.

[11] L. Debiasi, C. Rathgeb, U. Scherhag, A. Uhl, and C. Busch. PRNU-based Detection of Morphed Face Images. In *Proceedings of 6th International Workshop on Biometrics and Forensics (IWBF 2018)*, 2018.

[12] R. Raghavendra, K. B. Raja, and C. Busch. Detecting morphed face images. In *2016 IEEE 8th International Conference on Biometrics Theory, Applications and Systems (BTAS)*, pages 1–7, Sep. 2016.

[13] R. Raghavendra, K. B. Raja, S. Venkatesh, and C. Busch. Transferable deep-cnn features for detecting digital and print-scanned morphed face images. In *2017 IEEE Conference on Computer Vision and Pattern Recognition Workshops (CVPRW)*, pages 1822–1830, July 2017.

[14] R. Raghavendra, K. Raja, S. Venkatesh, and C. Busch. Face morphing versus face averaging: Vulnerability and detection. In *2017 IEEE International Joint Conference on Biometrics (IJCB)*, pages 555–563, Oct. 2017.

[15] Andrey Makrushin, Tom Neubert, and Jana Dittmann. Automatic generation and detection of visually faultless facial morphs. In *Proceedings of the 12th International Joint Conference on Computer Vision, Imaging and Computer Graphics Theory and Applications - Volume 6: VISAPP, (VISIGRAPP 2017)*, pages 39–50. INSTICC, SciTePress, 2017.

[16] T. Neubert, A. Makrushin, M. Hildebrandt, C. Kraetzer, and J. Dittmann. Extended stirtrace benchmarking of biometric and forensic qualities of morphed face images. *IET Biometrics*, 7(4):325–332, 2018.

[17] Matteo Ferrara, Annalisa Franco, and Davide Maltoni. *On the Effects of Image Alterations on Face Recognition Accuracy*, pages 195–222. Springer International Publishing, Cham, 2016.

[18] Paul Viola and Michael Jones. Rapid object detection using a boosted cascade of simple features. In *Proceedings of the 2001 IEEE Computer Society Conference on Computer Vision and Pattern Recognition. CVPR 2001*, 2001.

[19] V. Kazemi and J. Sullivan. One millisecond face alignment with an ensemble of regression trees. In *2014 IEEE Conference on Computer Vision and Pattern Recognition*, 2014.

[20] JTC 1/SC 37. International organization for standardization: Information technology biometric presentation attack detection part 3: Testing and reporting. In *ISO/IEC 30107-3*, 2017.

[21] E. J. Berg. *Heaviside's operational calculus as applied to engineering and physics*. Electrical engineering texts. McGraw-Hill book company, inc., 1936.